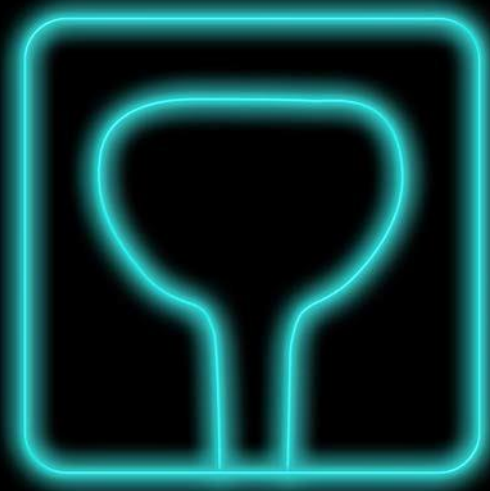


PI-RADS[®]

Prostate Imaging – Reporting
and Data System

2019
Version 2.1



ACR[®]
AMERICAN COLLEGE OF
RADIOLOGY
QUALITY IS OUR IMAGE

PI-RADS®

Prostate Imaging – Reporting and Data System

2019
Version 2.1



ACKNOWLEDGEMENTS

Administration

Mythreyi Chatfield
Lauren Hicks
Dipleen Kaur
Cassandra Vivian-Davis

American College of Radiology, Reston
American College of Radiology, Reston
American College of Radiology, Reston
American College of Radiology, Reston

Steering Committee

Jeffrey C. Weinreb: Co-Chair

Yale School of Medicine, New Haven

Jelle O. Barentsz: Co-Chair

Radboudumc, Nijmegen

Peter L. Choyke

National Institutes of Health, Bethesda

François Cornud

René Descartes University, Paris

Masoom A. Haider

University of Toronto, Sunnybrook Health Sciences Ctr

Katarzyna J. Macura

Johns Hopkins University, Baltimore

Daniel Margolis

University of California, Los Angeles

Mitchell D. Schnall

University of Pennsylvania, Philadelphia

Faina Shtern

AdMeTech Foundation

Clare M. Tempany

Harvard University, Boston

Harriet C. Thoeny

University Hospital of Bern

Baris Turkbey

National Institutes of Health, Bethesda

Andrew Rosenkrantz

NYU Langone Health

Geert Villeirs

Ghent University Hospital

Sadhna Verma

University of Cincinnati

DCE

Peter L. Choyke: Chair-DCE	National Institutes of Health, Bethesda
Aytekin Oto	University of Chicago
Masoom A. Haider	University of Toronto, Sunnybrook Health Sciences Center
Francois Cornud	Rene Descartes University, Paris
Fiona Fennessy	Harvard University, Boston
Sadhna Verma	University of Cincinnati
Pete Choyke	National Institutes of Health, Bethesda
Jurgen Fütterer	Radboudumc, Nijmegen

DWI

Francois Cornud: Chair	René Descartes University, Paris
Anwar Padhani	Mount Vernon Cancer Centre, Middlesex
Daniel Margolis	University of California, Los Angeles
Aytekin Oto	University of Chicago
Harriet C. Thoeny	University Hospital of Bern
Sadhna Verma	University of Cincinnati
Peter Choyke	National Institutes of Health, Bethesda
Jelle Barentsz	Radboudumc, Nijmegen
Masoom A. Haider	University of Toronto, Sunnybrook Health Sciences Ctr
Clare M. Tempany	Harvard University, Boston
Geert Villeirs	Ghent University Hospital
Baris Turkbey	National Institutes of Health, Bethesda

Sector Diagram

David A. Rini J	Johns Hopkins University
-----------------	--------------------------

Other Reviewers/Contributors

ESUR

Alex Kirkham	University College London Hospitals
Clare Allen	University College London Hospitals
Nicolas Grenier	University Boordeaux
Valeria Panebianco	Sapienza University of Rome
Mark Emberton	University College London Hospitals
Jonathan Richenberg	The Montefiore Hospital, Brighton
Tristan Barrett	University of Cambridge School of Clinical Medicine, UK
Vibeke Løgager	University of Copenhagen, Denmark
Bernd Hamm	Charité, Universitätsmedizin, Berlin, Germany
Philippe Puech	Lille University School of Medicine

USA

Martin Cohen	Rolling Oaks Radiology, California
John Feller	Desert Medical Imaging, Indian Wells, Ca
Daniel Cornfeld	Yale School of Medicine, New Haven
Art Rastinehad	Mount Sinai School of Medicine
John Leyendecker	University of Texas Southwestern Medical Center, Dallas
Ivan Pedrosa	University of Texas Southwestern Medical Center, Dallas
Andrei Purysko	Cleveland Clinic
Peter Humphey	Yale School of Medicine, New Haven
Preston Sprenkle	Yale School of Medicine, New Haven
Rajan Gupta	Duke University
Steven Raman	UCLA
Aytekın Oto	University of Chicago

Daniel Costa

University of Texas Southwestern Medical Center

Samir Taneja

NYU Langone Health

Peter Pinto

National Cancer Institute, Bethesda

Leonard Marks

UCLA

China

Liang Wang

Tongji Medical College

Australia

Les Thompson

Wesley Hospital, Brisbane

TABLE OF CONTENTS

INTRODUCTION.....	1
SECTION I: CLINICAL CONSIDERATIONS AND TECHNICAL SPECIFICATIONS	4
SECTION II: NORMAL ANATOMY AND BENIGN FINDINGS.....	7
SECTION III: ASSESSMENT AND REPORTING	10
SECTION IV: MULTIPARAMETRIC MRI (MPMRI)	17
SECTION V: STAGING	25
APPENDIX I	26
APPENDIX II.....	30
APPENDIX III.....	32
APPENDIX IV	41
APPENDIX V	42
REFERENCES	43
FIGURES.....	53

INTRODUCTION

Magnetic Resonance Imaging (MRI) has been used for noninvasive assessment of the prostate gland and surrounding structures since the 1980s. Initially, prostate MRI was based solely on morphologic assessment using T1-weighted (T1W) and T2-weighted (T2W) pulse sequences, and its role was primarily for locoregional staging in patients with biopsy proven cancer. However, it provided limited capability to distinguish benign pathological tissue and clinically insignificant prostate cancer from significant cancer.

Advances in technology (both in software and hardware) have led to the development of multiparametric MRI (mpMRI), which combines anatomic T2W imaging with functional and physiologic assessment, including diffusion-weighted imaging (DWI) and its derivative apparent-diffusion coefficient (ADC) maps, dynamic contrast-enhanced (DCE) MRI, and sometimes other techniques such as in-vivo MR proton spectroscopy. These technologic advances, combined with a growing interpreter experience with mpMRI, have substantially improved diagnostic capabilities for addressing the central challenges in prostate cancer care: 1) Improving detection of clinically significant cancer, which is critical for reducing mortality; and 2) Increasing confidence in benign diseases and dormant malignancies, which are not likely to cause morbidity in a man's lifetime, in order to reduce unnecessary biopsies and treatment.

Consequently, clinical applications of prostate MRI have expanded to include not only locoregional staging, but also tumor detection, localization (registration against an anatomical reference), characterization, risk stratification, surveillance, assessment of suspected recurrence, and image guidance for biopsy, surgery, focal therapy and radiation therapy.

In 2007, recognizing an important evolving role for MRI in assessment of prostate cancer, the AdMeTech Foundation organized the International Prostate MRI Working Group, which brought together key leaders of academic research and industry. Based on deliberations by this group, a research strategy was developed and a number of critical impediments to the widespread acceptance and use of MRI were identified. Amongst these was excessive variation in the performance, interpretation, and reporting of prostate MRI exams. A greater level of standardization and consistency was recommended in order to facilitate multi-center clinical evaluation and implementation.

In response, the European Society of Urogenital Radiology (ESUR) drafted guidelines, including a scoring system, for prostate MRI known as Prostate Imaging-Reporting and Data System version 1 (PI-RADS v1). Since it was published in 2012, PI-RADS v1 has been validated in certain clinical and research scenarios. However, experience has also revealed several limitations, in part due to rapid progress in the field. In an effort to make PI-RADS standardization more globally acceptable, the American College of Radiology (ACR), ESUR and the AdMeTech Foundation established a Steering Committee to build upon, update and improve upon the foundation of PI-RADS v1. This effort resulted in the development of PI-RADS v2.

PI-RADS v2 was developed by members of the PI-RADS Steering Committee, several working groups with international representation, and administrative support from the ACR using the best available evidence and expert consensus opinion. It is designed to promote global standardization and diminish variation in the acquisition, interpretation, and reporting of prostate mpMRI examinations,

and it is intended to be a “living” document that will evolve as clinical experience and scientific data accrue.

Following its initial release, numerous studies validated the value of PI-RADS v2, but, as expected, also showed some inconsistencies and limitations. For example, inter-observer agreement was good to moderate, and a number of specific assessment criteria were identified that required clarification or adjustment. Furthermore, certain technical issues concerning the acquisition of mpMRI data warranted updating and refinement. To address these issues, the PI-RADS Steering Committee, again using a consensus-based process, recommended several modifications to PI-RADS v2, maintaining the framework of assigning scores to individual sequences and using these scores to derive an overall assessment category. The updated version is termed PI-RADS v2.1.

PI-RADS v2.1 is designed to improve detection, localization, characterization, and risk stratification in patients with suspected cancer in treatment naïve prostate glands. The overall objective is to improve outcomes for patients. The specific aims are to:

- Establish minimum acceptable technical parameters for prostate mpMRI
- Simplify and standardize the terminology and content of radiology reports
- Facilitate the use of MRI data for targeted biopsy
- Develop assessment categories that summarize levels of suspicion or risk and can be used to select patients for biopsies and management (e.g., observation strategy vs. immediate intervention)
- Enable data collection and outcome monitoring
- Educate radiologists on prostate MRI reporting and reduce variability in imaging interpretations
- Enhance interdisciplinary communications with referring clinicians

PI-RADS v2.1 is not a comprehensive prostate cancer diagnosis document and should be used in conjunction with other current resources. For example, it does not address the use of MRI for detection of suspected recurrent prostate cancer following therapy, progression during surveillance, or the use of MRI for evaluation of other parts of the body (e.g. skeletal system) that may be involved with prostate cancer. Furthermore, it does not elucidate or prescribe optimal technical parameters; only those that should result in an acceptable mpMRI examination.

The PI-RADS Steering Committee strongly supports the continued development of promising MRI methodologies for assessment of prostate cancer and local staging (e.g. nodal metastases) utilizing novel and/or advanced research tools not included in PI-RADS v2.1, such as in-vivo MR spectroscopic imaging (MRSI), diffusion tensor imaging (DTI), diffusional kurtosis imaging (DKI), multiple b-value assessment of fractional ADC, intravoxel incoherent motion (IVIM), blood oxygenation level dependent (BOLD) imaging, intravenous ultra-small superparamagnetic iron oxide (USPIO) agents, and MR-PET. Consideration will be given to incorporating them into future versions of PI-RADS as relevant data and experience become available.

SECTION I: CLINICAL CONSIDERATIONS AND TECHNICAL SPECIFICATIONS

A. Clinical Considerations

1. Timing of MRI Following Prostate Biopsy

Hemorrhage, manifested as hyperintense signal on T1W, may be present in the prostate gland, most commonly the peripheral zone (PZ) and seminal vesicles, following systematic transrectal ultrasound-guided systematic (TRUS) biopsy and may confound mpMRI assessment. When there is evidence of hemorrhage in the PZ on MR images, consideration may be given to postponing the MRI examination until a later date when hemorrhage has resolved. However, this may not always be feasible or necessary, and clinical practice may be modified as determined by individual circumstances and available resources. Furthermore, if the MRI exam is performed following a negative TRUS biopsy, the likelihood of clinically significant prostate cancer at the site of post biopsy hemorrhage without a corresponding suspicious finding on MRI is low. In this situation, a clinically significant cancer, if present, is likely to be in a location other than that with blood products. Thus, the detection of clinically significant cancer is not likely to be substantially compromised by post biopsy hemorrhage, and there may be no need to delay MRI after prostate biopsy if the primary purpose of the exam is to detect and characterize clinically significant cancer in the gland.

However, post biopsy changes, including hemorrhage and inflammation, may adversely affect the interpretation of prostate MRI for staging in some instances. Although these changes may persist for many months, they tend to diminish over time, and an interval of at least 6 weeks or longer between biopsy and MRI should be considered.

2. Patient Preparation

At present, there is no consensus concerning all patient preparation issues.

To reduce motion artifact from bowel peristalsis, the use of an antispasmodic agent (e.g. glucagon, scopolamine butylbromide, or sublingual hyoscyamine sulfate) may be beneficial in some patients. However, in many others it is not necessary, and the incremental cost and potential for adverse drug reactions should be taken into consideration.

The presence of stool in the rectum may interfere with placement of an endorectal coil (ERC). If an ERC is not used, the presence of air and/or stool in the rectum may induce artifactual distortion that can compromise DWI quality. Thus, some type of minimal preparation enema administered by the patient in the hours prior to the exam may be beneficial, especially if the exam is performed without an ERC. However, an enema may also promote peristalsis, resulting in increased motion related artifacts in some instances.

The patient should evacuate the rectum, if possible, just prior to the MRI exam.

Some recommend that patients refrain from ejaculation for three days prior to the MRI exam in order to maintain maximum distention of the seminal vesicles. However, a benefit for assessment of the prostate and seminal vesicles for clinically significant cancer has not been firmly established.

3. Patient Information

The following information should be available to the radiologist at the time of MRI exam performance and interpretation:

- Recent serum prostate-specific antigen (PSA) level and PSA history
- Date and results of prostate biopsy, including number of cores, locations and Gleason scores of positive biopsies (with % core involvement when available)
- Other relevant clinical history, including digital rectal exam (DRE) findings, medications (particularly in the setting of alpha blockers, hormones/hormone ablation), prior prostate infections, pelvic surgery, radiation therapy, and family history.

B. Technical Specifications

Prostate MRI acquisition protocols should always be tailored to specific patients, clinical questions, management options, and MRI equipment. Unless the MRI exam is monitored and no findings suspicious for clinically significant prostate cancer are detected, at least one pulse sequence should use a field-of-view (FOV) that permits evaluation of pelvic lymph nodes to the level of the aortic bifurcation. The supervising radiologist should be cognizant that superfluous or inappropriate sequences unnecessarily increase exam time and discomfort, and this could negatively impact patient acceptance and compliance.

The technologist performing the exam and/or supervising radiologist should monitor the scan for quality control. If image quality of a pulse sequence is compromised due to patient motion or other reason, measures should be taken to rectify the problem and the sequence should be repeated.

1. Magnetic Field Strength

The fundamental advantage of 3T compared with 1.5T lies in an increased signal-to-noise ratio (SNR), which theoretically increases linearly with the static magnetic field. This may be exploited to increase spatial resolution, temporal resolution, or both. Depending on the pulse sequence and specifics of implementation, power deposition, artifacts related to susceptibility, and signal heterogeneity could increase at 3T, and techniques that mitigate these concerns may result in some increase in imaging time and/or decrease in SNR. However, current state-of-the-art 3T MRI scanners can successfully address these issues, and most members of the PI-RADS Steering Committee agree that the advantages of 3T substantially outweigh these concerns.

There are many other factors that affect image quality besides magnetic field strength, and both 1.5T and 3.0T can provide adequate and reliable diagnostic exams when acquisition parameters are optimized and appropriate contemporary technology is employed. Although prostate MRI at both 1.5T and 3T has been well established, most members of the PI-RADS Steering Committee prefer, use, and recommend 3T for prostate MRI. When a patient has an implanted device that has been determined to be MR conditional at 1.5T but not at 3T, 1.5T should be considered. Additionally, 1.5T may be preferred when patients are safe to undergo MRI at 3T but the location of an implanted device may result in artifact that could compromise image quality (e.g., bilateral metallic hip prosthesis).

The recommendations in this document focus only on 3T and 1.5T MRI scanners since they have been the ones used for clinical validation of mpMRI. Prostate mpMRI at lower magnetic field strengths (<1.5T) is not recommended unless adequate peer reviewed clinical validation becomes available.

2. Endorectal Coil (ERC)

When integrated with external (surface) phased array coils, endorectal coils (ERCs) increase SNR in the prostate at any magnetic field strength. This may be particularly valuable for high spatial resolution imaging used in cancer staging and for inherently lower SNR sequences, such as DWI and high temporal resolution DCE.

ERCs can also be advantageous for larger patients where the SNR in the prostate may be compromised using only external phased array RF coils. However, use of an ERC may increase the cost and time of the examination, deform the gland, and introduce artifacts. In addition, it may be uncomfortable for patients and increase their reluctance to undergo MRI.

With some 1.5T MRI systems, especially older ones, use of an ERC is considered indispensable for achieving the type of high resolution diagnostic quality imaging needed for staging prostate cancer. At 3T without use of an ERC, image quality can be comparable with that obtained at 1.5 T with an ERC, although direct comparison of both strategies for cancer detection and/or staging is lacking. Importantly, there are many technical factors other than the use of an ERC that influence SNR (e.g. receiver bandwidth, coil design, efficiency of the RF chain), and some contemporary 1.5T scanners that employ a relatively high number of external phased array coil elements and RF channels (e.g. 16 or more) may be capable of achieving adequate SNR in many patients without an ERC.

Credible satisfactory results have been obtained at both 1.5T and 3T without the use of an ERC. Taking these factors into consideration as well as the variability of MRI equipment available in clinical use, the PI-RADS Steering Committee recommends that supervising radiologists strive to optimize imaging protocols in order to obtain the best and most consistent image quality possible with the MRI scanner used. However, cost, availability, patient preference, and other considerations cannot be ignored.

If air is used to inflate the ERC balloon, it may introduce local magnetic field inhomogeneity, resulting in distortion on DWI, especially at 3T. The extent to which artifacts interfere with MRI interpretation will vary depending on specific pulse sequence implementations, but they can be diminished using correct positioning of the ERC and distention of the balloon with liquids (e.g. liquid perfluorocarbon or barium suspension) that will not result in susceptibility artifacts. When liquid is used for balloon distention, all air should be carefully removed from the ERC balloon prior to placement. Solid, rigid reusable ERCs that avoid the need for inflatable balloons and decrease gland distortion have been developed.

3. Computer-Aided Evaluation (CAE) Technology

Computer-aided evaluation (CAE) technology using specialized software or a dedicated workstation is not required for prostate mpMRI interpretation. However, CAE may improve workflow (display, analysis, interpretation, reporting, and communication), provide quantitative pharmacodynamic data, and enhance lesion detection and discrimination performance for some radiologists, especially those with less experience interpreting mpMRI exams. CAE can also facilitate integration of MRI data with some forms of MR targeted biopsy systems.

SECTION II: NORMAL ANATOMY AND BENIGN FINDINGS

A. Normal Anatomy

From superior to inferior, the prostate consists of the base (just below the urinary bladder), the midgland, and the apex. It is divided into four histologic zones: (a) the anterior fibromuscular stroma, contains no glandular tissue; (b) the transition zone (TZ), surrounding the urethra proximal to the verumontanum, contains 5% of the glandular tissue; (c) the central zone (CZ), surrounding the ejaculatory ducts, contains about 20% of the glandular tissue; and (d) the outer peripheral zone (PZ), contains 70%–80% of the glandular tissue. When benign prostatic hyperplasia (BPH) develops, the TZ will account for an increasing percentage of the gland volume.

Approximately 70-75% of prostate cancers originate in the PZ and 20-30% in the TZ. Cancers originating in the CZ are uncommon, and the cancers that occur in the CZ are usually secondary to invasion by PZ tumors.

Based on location and differences in signal intensity on T2W images, the TZ can often be distinguished from the CZ on MR images. However, in some patients, age-related expansion of the TZ by BPH may result in compression and displacement of the CZ. Use of the term “central gland” to refer to the combination of TZ and CZ is discouraged as it is not reflective of the zonal anatomy as visualized or reported on pathologic specimens.

A thin, dark rim partially surrounding the prostate on T2W is often referred to as the “prostate capsule”. It serves as an important landmark for assessment of extraprostatic extension of cancer. In fact, the prostate lacks a true capsule; rather it contains an outer band of concentric fibromuscular tissue that is inseparable from prostatic stroma. It is incomplete anteriorly and apically.

The prostatic pseudocapsule (sometimes referred to as the “surgical capsule”) on T2W MRI is a thin, dark rim at the interface of the TZ with the PZ. There is no true capsule in this location at histological evaluation, and this appearance is due to compressed prostate tissue.

Nerves that supply the corpora cavernosa are intimately associated with arterial branches from the inferior vesicle artery and accompanying veins that course posterolateral at 5 and 7 o'clock to the prostate bilaterally, and together they constitute the neurovascular bundles. At the apex and base, small nerve branches surround the prostate periphery and penetrate through the capsule, a potential route for extraprostatic extension (EPE) of cancer.

B. Sector Map (Appendix II)

The segmentation model used in PI-RADS v2.1 was adapted from a European Consensus Meeting and the ESUR Prostate MRI Guidelines 2012. It employs forty-one sectors/regions: thirty-eight for the prostate, two for the seminal vesicles and one for the external urethral sphincter (Appendix II).

Use of the Sector Map will enable radiologists, urologists, pathologists, and others to localize findings described in MRI reports, and it will be a valuable visual aid for discussions with patients about biopsy and treatment options.

Division of the prostate and associated structures into sectors standardizes reporting and facilitates precise localization for MR-targeted biopsy and therapy, pathological correlation, and research. Since relationships between tumor contours, glandular surface of the prostate, and adjacent structures, such as neurovascular bundles, external urethral sphincter, and bladder neck, are valuable information for periprostatic tissue sparing surgery, the Sector Map may also provide a useful roadmap for surgical dissection at the time of radical prostatectomy.

Either hardcopy (on paper) or electronic (i.e. on computer) recording on the Sector Map is acceptable.

For information about the use of the Sector Map, see Section III and Appendix II.

C. Benign Findings

Many signal abnormalities within the prostate are benign. The most common include:

1. Benign prostatic hyperplasia (BPH)

Benign prostatic hyperplasia (BPH) develops in response to testosterone, after it is converted to dihydrotestosterone. BPH arises in the TZ, although exophytic and extruded BPH nodules can be found in the PZ or CZ. BPH consists of a mixture of stromal and glandular hyperplasia and may appear as band-like areas and/or encapsulated round nodules with circumscribed or encapsulated margins. Predominantly glandular BPH nodules and cystic atrophy exhibit moderate-marked T2 hyperintensity and are distinguished from malignant tumors by their signal and capsule. Predominantly stromal nodules exhibit T2 hypointensity. Many BPH nodules demonstrate a mixture of signal intensities. BPH nodules may be highly vascular on DCE and can demonstrate a range of signal intensities on DWI.

Although BPH is a benign entity, it may have important clinical implications for biopsy approach and therapy since it can increase gland volume, stretch the urethra, and impede the flow of urine. Since BPH tissue produces prostate-specific antigen (PSA), accurate measurement of gland volume by MRI is an important metric to allow correlation with an individual's PSA level and to calculate the PSA density (PSA/prostate volume).

2. Hemorrhage

Hemorrhage in the PZ and/or seminal vesicles is common after biopsy. It appears as focal or diffuse hyperintense signal on T1W and iso-hypointense signal on T2W. However, chronic blood products may appear hypointense on all MR sequences.

3. Cysts

A variety of cysts can occur in the prostate and adjacent structures. As elsewhere in the body, cysts in the prostate may contain "simple" fluid and appear markedly hyperintense on T2W and dark on T1W. However, they can also contain blood products or proteinaceous fluid, which may demonstrate a variety of signal characteristics, including hyperintense signal on T1W.

4. Calcifications

Calcifications, if visible, appear as markedly hypointense foci (e.g. signal voids) on all pulse sequences

5. Prostatitis

Prostatitis affects many men, although it is often sub-clinical. Pathologically, it presents as an immune infiltrate, the character of which depends on the agent causing the inflammation. On MRI, prostatitis can result in decreased signal in the PZ on both T2W and the ADC (apparent diffusion coefficient) map. Prostatitis may also increase perfusion, resulting in a “false positive” DCE result. However, the morphology is commonly band-like, wedge-shaped, or diffuse rather than focal, round, oval, or irregular, and the decrease in signal on the ADC map is generally not as pronounced nor as focal as in cancer.

6. Atrophy

Prostatic atrophy can occur as a normal part of aging or from chronic inflammation. It is typically associated with wedge-shaped areas of low signal on T2W and mildly decreased signal on the ADC map from loss of glandular tissue. The ADC is generally not as low as in cancer, and there is often contour retraction of the involved prostate.

7. Fibrosis

Prostatic fibrosis can occur after inflammation. It may be associated with wedge- or band-shaped areas of low signal on T2W.

SECTION III: ASSESSMENT AND REPORTING

A major objective of a prostate MRI exam is to identify and localize abnormalities that correspond to clinically significant prostate cancer, and mpMRI is able to detect intermediate to high grade cancers with volumes <5mm, depending on the location and background tissue within the prostate gland. However, there is no universal agreement of the definition of clinically significant prostate cancer.

In PI-RADS™ v2.1, the definition of clinically significant cancer is intended to standardize reporting of mpMRI exams and correlation with pathology for clinical and research applications. Based on the current uses and capabilities of mpMRI and MRI-targeted procedures, for PI-RADS v2.1 clinically significant cancer is defined on pathology/histology as Gleason score ≥ 7 (including 3+4 with prominent but not predominant Gleason 4 component), and/or volume ≥ 0.5 cc, and/or extraprostatic extension (EPE).

PI-RADS™ v2.1 assessment uses a 5-point scale based on the likelihood (probability) that a combination of mpMRI findings on T2W, DWI, and DCE correlates with the presence of a clinically significant cancer for each lesion in the prostate gland.

PI-RADS™ v2.1 Assessment Categories

PI-RADS 1 – Very low (clinically significant cancer is highly unlikely to be present)

PI-RADS 2 – Low (clinically significant cancer is unlikely to be present)

PI-RADS 3 – Intermediate (the presence of clinically significant cancer is equivocal)

PI-RADS 4 – High (clinically significant cancer is likely to be present)

PI-RADS 5 – Very high (clinically significant cancer is highly likely to be present)

Assignment of a PI-RADS™ v2.1 Assessment Category should be based on mpMRI findings only and should not incorporate other factors such as serum prostate specific antigen (PSA), digital rectal exam, or clinical history, or planned treatments. Although biopsy should be considered for PI-RADS 4 or 5, but not for PI-RADS 1 or 2, PI-RADS v2.1 does not include recommendations for management, as these must take into account other factors besides the MRI findings, including laboratory/clinical history and local preferences, expertise and standards of care. Thus, for findings with PI-RADS Assessment Category 3, biopsy may or may not be appropriate, depending on factors other than mpMRI alone.

It is anticipated that, as evidence continues to accrue in the field of mpMRI and MRI-targeted biopsies and interventions, specific recommendations and/or algorithms regarding biopsy and management will be included in future versions of PI-RADS™.

When T2W and DWI are of diagnostic quality, DCE plays a minor role in determining PI-RADS Assessment Category. Absence of early enhancement within a lesion usually adds little information, and diffuse enhancement not localized to a specific T2W or DWI abnormality can be seen in the setting of prostatitis. Moreover, DCE does not contribute to the overall assessment when the finding has a low (PI-RADS 1 or 2) or high (PI-RADS 4 or 5) likelihood of clinically significant cancer. However, when DWI is PI-RADS 3 in the PZ, a positive DCE may increase the likelihood that the finding corresponds to a clinically significant cancer and may upgrade the Assessment Category to PI-RADS 4.

PI-RADS Assessment

Peripheral Zone (PZ)

DWI	T ₂ W	DCE	PI-RADS
1	Any*	Any	1
2	Any	Any	2
3	Any	–	3
		+	4
4	Any	Any	4
5	Any	Any	5

* "Any" indicates 1-5

Transition Zone (TZ)

T ₂ W	DWI	DCE	PI-RADS
1	Any*	Any	1
2	≤3	Any	2
	≥4	Any	3
3	≤4	Any	3
	5	Any	4
4	Any	Any	4
5	Any	Any	5

* "Any" indicates 1-5

A. Reporting (see Appendix I: Report Templates)

Measurement of the Prostate Gland

The volume of the prostate gland should always be reported. It may be determined using manual or automated segmentation or calculated using ellipsoid formulation; (maximum AP dimension) x (maximum longitudinal dimension) [both placed on the mid-sagittal T2W image] x (maximum transverse dimension) [placed on the axial T2W image] x 0.52.

Prostate volume may also be useful to calculate PSA density (PSAD=PSA/prostate volume reported in ng/ml²)

Mapping Lesions

Prostate cancer is often multifocal. The largest tumor focus usually yields the highest Gleason score and is most likely to contribute to extraprostatic extension (EPE) and positive surgical margins.

For PI-RADS™ v2.1, up to four lesions with a PI-RADS Assessment Category of 3, 4, or 5 may each be assigned on the Sector Map (Appendix II), and the index (dominant) intraprostatic lesion should be identified. The index lesion is the one with the highest PI-RADS Assessment Category. If the highest PI-RADS Assessment Category is assigned to two or more lesions, the index lesion should be the one that shows EPE. Thus, a smaller lesion with EPE should be defined as the index lesion despite the presence of a larger tumor with the identical PI-RADS Assessment Category. If none of the lesions demonstrate EPE, the largest of the tumors with the highest PI-RADS Assessment Category should be considered the index lesion.

If there are more than four suspicious lesions, then only the four with the highest likelihood of clinically significant cancer (i.e. highest PI-RADS Assessment Category) should be reported. There may be instances when it is appropriate to report more than four suspicious lesions.

Reporting of additional findings with PI-RADS Assessment Category 2 or definitely benign findings (e.g. cyst) is optional, but may be helpful to use as landmarks to guide subsequent biopsy or for tracking lesions on subsequent mpMRI exams.

If a suspicious finding extends beyond the boundaries of one sector, all neighboring involved sectors should be indicated on the Sector Map (as a single lesion).

Measurement of Lesions

With current techniques, mpMRI has been shown to underestimate both tumor volume and tumor extent compared to histology, especially for Gleason grade 3. Furthermore, the most appropriate imaging plane and pulse sequence for measuring lesion size on MRI has not been definitely determined, and the significance of differences in lesion size on the various MRI pulse sequences requires further investigation. In the face of these limitations, the PI-RADS Steering Committee nevertheless believes that standardization of measurements will facilitate MR-pathological correlation and research and recommends that the following rules be used for measurements.

The minimum requirement is to report the largest dimension of a suspicious lesion on an axial image. If the largest dimension of a suspicious lesion is on sagittal and/or coronal images, this measurement and imaging plane should also be reported. If a lesion is not clearly delineated on an axial image, report the measurement on the image which best depicts the finding.

Alternatively, if preferred, lesion volume may be determined using appropriate software, or three dimensions of lesions may be measured so that lesion volume may be calculated (max a-p diameter x max l-r diameter x max c-c diameter x 0.52).

In the PZ, lesions should be measured on ADC. In the TZ, lesions should be measured on T2W.

If lesion measurement is difficult or compromised on ADC (for PZ) or T2W (for TZ), measurement should be made on the sequence that shows the lesion best.

In the mpMRI report, the image number(s)/series and sequence used for measurement should be indicated.

Evaluation of lesions in specific anatomic regions of the prostate

Evaluation of the TZ

BPH manifests as a varying number of hyperplastic nodules and intervening tissue in the TZ in almost all men undergoing MRI for assessment of prostate cancer. Often, it is challenging on MRI to determine which, if any, findings in such a background should be scored and assigned a PI-RADS assessment category. PI-RADS v2.1 advises that the shape and margin features of TZ findings should be assessed in at least two planes on T2W MRI using the described TZ assessment criteria.

What to Score in the TZ: Focal lesions, nodules, or regions in the TZ with features known to be associated with malignancy on T2W or DWI and that differ from the predominant imaging characteristics of the background should be scored. For example, a lesion/region between nodules with more restricted diffusion than background, or a nodule with clearly more restricted diffusion than the background (on high b-value images and ADC maps) should be scored. A focal lesion that is different from other (background) nodules in having obscured margins, lenticular shape, or invasive behavior on T2W images should also be scored, even if without differing restricted diffusion compared to background, should also be scored.

Other findings should not be scored. For example, if there is restricted diffusion in multiple, similar appearing nodules scattered throughout the TZ, thus making restricted diffusion a feature of the background, these should not be scored.

How to Score in the TZ: The T2W score is the dominant factor that determines the PI-RADS assessment category in the TZ, and a T2W score of 1 indicates a normal appearance of the TZ. Since MRI findings of age-related BPH are present in the TZ in almost all men undergoing prostate mpMRI for the assessment of csPCa, and typical BPH nodules are highly unlikely to harbor csPCA, findings of BPH alone are considered a normal variant and should be assigned a T2W score of 1. These types of nodules do not have to be separately reported. Since every MRI exam should be assigned a PI-RADS assessment category 1-5, when there are no findings with a PI-RADS assessment category >1, the overall PI-RADS assessment category for the MRI exam should be reported as PI-RADS 1: clinically significant cancer is highly unlikely.

When circumscribed nodules in the TZ are incompletely or almost completely encapsulated, these atypical nodules are assigned a T2W score of 2.

Although the T2W score is the dominant factor that determines the PI-RADS assessment category in the TZ, restricted diffusion is also a feature of malignancy. Occasionally, atypical nodules in the TZ may contain cancer, and DWI may be helpful to identify them. Given the increased likelihood of PCa associated with high DWI scores in atypical TZ nodules, atypical TZ nodules (T2W score of 2) are upgraded to PI-RADS assessment category 3 if they have a DWI score of >4 (i.e., with markedly

restricted diffusion).

Mildly/moderately restricted diffusion is commonly encountered in mostly encapsulated and unencapsulated lesions in the TZ. Such lesions may represent areas of stromal hyperplasia and should not be upgraded on the basis of mildly/moderately restricted diffusion. Therefore, findings with a T2W score of 1 or 2 should not be upgraded to a PI-RADS assessment category of 2 or 3, respectively, based on a DWI score of a 3 (i.e., mildly/moderately restricted diffusion).

Evaluation of the central zone

The normal CZ is usually visible on T2W and ADC images as bilaterally symmetric low signal intensity tissue encircling the ejaculatory ducts from the prostatic base to the verumontanum. It is symmetrically, mildly hyperintense on high b-value DWI, and it does not demonstrate early enhancement nor asymmetric increased signal intensity on high b-value DWI. PCa originating in the CZ is uncommon, and most of these arise in either the adjacent PZ or TZ and extend into the CZ. Focal early enhancement and/or asymmetry between the right and left CZ on T2W, ADC or high b-value images are findings that may indicate the presence of PCa. However, asymmetry in size alone may be a normal variant, especially in the setting of benign prostatic hyperplasia (BPH) in the TZ, which may deform, displace or cause asymmetry of the CZ. Occasionally, the normal CZ may appear as a discrete nodule in the midline above the level of the verumontanum; symmetric signal on ADC/DWI images and/or lack of early contrast enhancement may help differentiate benign from malignant tissue.

Evaluation of the anterior fibromuscular stroma (AFMS)

The normal AFMS shows bilaterally symmetric shape ("crescentic") and symmetric low signal intensity (similar to that of obturator or pelvic floor muscles) on T2W, ADC, and high b-value DWI without early enhancement. Abnormalities with increased T2W signal intensity relative to the pelvic muscles, with high signal intensity on high b-value DWI, low signal on ADC compared to adjacent pelvic muscle signal intensity (and hence relatively lower signal on ADC than normal AFMS), asymmetric enlargement or focal mass, and early enhancement may all be helpful to detect PCa that has extended into the AFMS. Since PCa does not originate in the AFMS, when reporting a suspicious lesion in the AFMS, criteria for either the PZ or TZ should be applied, depending on the zone from which the lesion appears most likely to be originating. It is understood that the zone of origin is not always certain, an inevitable limitation of PI-RADS assessment methodology.

Caveats for Overall Assessment

- In order to facilitate correlation and synchronized scrolling when viewing, it is strongly recommended that imaging plane angle, location, and slice thickness for all sequences (T2W, DWI, and DCE) are identical.
- Changes from prostatitis (including granulomatous prostatitis) can cause signal abnormalities in the PZ with all pulse sequences. Morphology and signal intensity may be helpful to stratify the likelihood of malignancy. In the PZ, mild signal changes on T2W and/or DWI that are not rounded but rather indistinct, linear, lobar, or diffuse are less likely to be malignant.
- For the PZ, DWI is the primary determining sequence (dominant technique). Thus, if the DWI score is 4 and T2W score is 2, PIRADS Assessment Category should be 4.
- For the TZ, T2W is the primary determining sequence. Thus, if the T2W score is 4 and DWI score is 2, PIRADS Assessment Category should be 4.

- Since the dominant sequences for PI-RADS assessment are T2W for the TZ and DWI for the PZ, identification of the zonal location of a lesion is vital. Areas where this may be especially problematic include the interface of the CZ and PZ at the base of the gland and the interface of the anterior horn of the PZ with TZ and anterior fibromuscular stroma (AFMS).
- Currently, the capability of reliably detecting and characterizing clinically significant prostate cancer with mpMRI in the TZ is less than that in the PZ.
- Homogeneous or heterogeneous nodules in the TZ that are round/oval, well-circumscribed, and encapsulated are common findings as men aged 40 and above. Often, they demonstrate restricted diffusion and/or focal contrast enhancement, but they are considered to be BPH. These do not have to be assigned a PI-RADS Assessment Category. Although such nodules may on occasion contain clinically significant prostate cancer, the probability is very low.
- Bilateral symmetric signal abnormalities on any sequence are often due to normal anatomy or benign changes.
- If a component of the mpMRI exam (T2W, DWI, DCE) is technically inadequate or was not performed, it should be assigned PI-RADS Assessment Category "X" for that component. This occurs most commonly with DWI. Since DWI is often crucial for diagnosis of clinically significant cancers in the PZ, inadequate or absent DWI data should usually prompt repeat of this component of the mpMRI examination if the cause of failure can be remedied. If this is not possible, assessment may be accomplished with the other pulse sequences that were obtained using the tables below. However, this is a substantial limitation, and it should be clearly acknowledged in the exam report, even if it applies to only one area of the prostate gland.

Assessment Without Adequate DWI

Peripheral Zone (PZ) and Transition Zone (TZ)

T ₂ W	DWI	DCE	PI-RADS
1	X	Any	1
2	X	Any	2
3	X	–	3
		+	4
4	X	Any	4
5	X	Any	5

Assessment Without Adequate DCE

Peripheral Zone (PZ): Determined by DWI Assessment Category

Transition Zone (TZ)

T ₂ W	DWI	DCE	PI-RADS
1	Any	X	1
2	≤3	X	2
	≥4	X	3
3	≤4	X	3
	5	X	4
4	Any	X	4
5	Any	X	5

If both DWI and DCE are inadequate or absent, assessment should be limited to staging for determination of EPE.

SECTION IV: MULTIPARAMETRIC MRI (MPMRI)

A. T1-Weighted (T1W) and T2-Weighted (T2W)

Both T1W and T2W sequences should be obtained for all prostate MR exams. T1W images are used primarily to determine the presence of hemorrhage within the prostate and seminal vesicles and to delineate the outline of the gland. T1W images may also be useful for detection of nodal and skeletal metastases, especially following intravenous administration of a gadolinium-based contrast agent (GBCA).

T2W images are used to discern prostatic zonal anatomy, assess abnormalities within the gland, and to evaluate for seminal vesicle invasion, EPE, and nodal involvement.

On T2W images, clinically significant cancers in the PZ usually appear as round or ill-defined hypointense focal lesions. However, this appearance is not specific and can be seen in various conditions such as prostatitis, hemorrhage, glandular atrophy, benign hyperplasia, biopsy related scars, and after therapy (hormone, ablation, etc.).

The T2W features of TZ tumors include non-circumscribed homogeneous, moderately hypointense lesions ("erased charcoal" or "smudgy fingerprint" appearance), spiculated margins, lenticular shape, absence of a complete hypointense capsule, and invasion of the urethral sphincter and anterior fibromuscular stroma. The more features present, the higher the likelihood of a clinically significant TZ cancer.

TZ cancers may be difficult to identify on T2W images since the TZ is often composed of variable amounts of glandular (T2-hyperintense) and stromal (T2-hypointense) tissue intermixed with each other, thus demonstrating heterogeneous signal intensity. Areas where benign stromal elements predominate may mimic or obscure clinically significant cancer.

Both PZ and TZ cancers may extend across anatomical boundaries. Invasive behavior is noted when there is extension within the gland (i.e. across regional parts of the prostate), into the seminal vesicles, or outside the gland (EPE).

1. Technical Specifications

T2W

T2W images should always be obtained in the axial plane (either straight axial to the patient or in an oblique axial plane matching the long axis of the prostate) and a minimum of one additional orthogonal plane (i.e., sagittal and/or coronal). T2W images are usually obtained with 2D RARE (rapid acquisition with relaxation enhancement) pulse sequences, more commonly known as fast-spin-echo (FSE) or turbo-spin-echo (TSE). In order to avoid blurring, excessive echo train lengths should be avoided.

- Slice thickness: 3mm, no gap. Imaging planes should be the same as those used for DWI and DCE
- FOV: generally 12-20 cm to encompass the entire prostate gland and seminal vesicles

- In plane dimension: ≤ 0.7 mm (phase) x ≤ 0.4 mm (frequency)

3D axial acquisitions may be used as an adjunct to 2D acquisitions. If acquired using isotropic voxels, 3D acquisitions may be particularly useful for visualizing detailed anatomy and distinguishing between genuine lesions and partial volume averaging effects. However, the soft tissue contrast is not identical and in some cases may be inferior to that seen on 2D T2W images, and the in-plane resolution may be lower than their 2D counterpart.

T1W

Axial T1W images of the prostate may be obtained with or without fat suppression using spin echo or gradient echo sequences. Locations should be the same as those used for DWI and DCE, although lower spatial resolution compared to T2W may be used to decrease acquisition time or increase anatomic coverage.

2. PI-RADS Assessment for T2W

Score	Peripheral Zone (PZ)
1	Uniform hyperintense signal intensity (normal)
2	Linear or wedge-shaped hypointensity or diffuse mild hypointensity, usually indistinct margin
3	Heterogeneous signal intensity or non-circumscribed, rounded, moderate hypointensity Includes others that do not qualify as 2, 4, or 5
4	Circumscribed, homogenous moderate hypointense focus/mass confined to prostate and <1.5 cm in greatest dimension
5	Same as 4 but ≥ 1.5 cm in greatest dimension or definite extraprostatic extension/invasive behavior
Score	Transition Zone (TZ)
1	Normal appearing TZ (rare) or a round, completely encapsulated nodule. ("typical nodule")
2	A mostly encapsulated nodule OR a homogeneous circumscribed nodule without encapsulation. ("atypical nodule") OR a homogeneous mildly hypointense area between nodules
3	Heterogeneous signal intensity with obscured margins Includes others that do not qualify as 2, 4, or 5
4	Lenticular or non-circumscribed, homogeneous, moderately hypointense, and <1.5 cm in greatest dimension
5	Same as 4, but ≥ 1.5 cm in greatest dimension or definite extraprostatic extension/invasive behavior

B. Diffusion-Weighted Imaging (DWI)

Diffusion-weighted imaging (DWI) reflects the random motion of water molecules and is a key component of the prostate mpMRI exam. It should include an ADC map and high b-value images.

The **ADC map** is a display of ADC values for each voxel in an image. In most current clinical implementations, it uses two or more b-values and a monoexponential model of signal decay with increasing b-values to calculate ADC values. Most clinically significant cancers have restricted/impeded diffusion compared to normal tissues and, thus, appear hypointense on grey-scale ADC maps. Although ADC values have been reported to correlate inversely with histologic grades, there is considerable overlap between BPH, low grade cancers, and high grade cancers. Furthermore, ADC calculations are influenced by choice of b-values and have been inconsistent across vendors. Thus, qualitative visual assessment is often used as the primary method to assess ADC. Nevertheless, ADC values, using a threshold of 750-900 $\mu\text{m}^2/\text{sec}$, may assist differentiation between benign and malignant prostate tissues, with ADC values below the threshold correlating with clinically significant cancers.

“High b-value” images utilize a b-value of at least 1400 sec/mm^2 . They display preservation of signal in areas of restricted/impeded diffusion compared with normal tissues, which demonstrate diminished signal due to greater diffusion between application of gradients with different b-values. Compared to ADC maps alone, conspicuity of clinically significant cancers is sometimes improved on high b-value images, especially in those adjacent to or invading the anterior fibromuscular stroma, in a subcapsular location, and at the apex and base of the gland. High b-value images can be obtained in one of two ways: either directly by acquiring a high b-value DWI sequence (requiring additional scan time), or by calculating (synthesizing) the high b-value image by extrapolation from the acquired lower b-value data used to create the ADC map (potentially less prone to artifacts because it avoids the longer TEs required to accommodate the strong gradient pulses needed for high b-value acquisitions). As the b-value increases, the signal-to-noise ratio (SNR) decreases, so that the optimum high b-value may be dependent on magnetic field strength, software, and manufacturer. Thus, there is no currently widely accepted optimal “high b-value” beyond the requirement for a DW image set with a b-value $\geq 1,400 \text{ sec}/\text{mm}^2$.

1. Technical Specifications

Free-breathing spin echo EPI sequence combined with spectral fat saturation is recommended.

- TE: $\leq 90 \text{ msec}$; TR: $\geq 3000 \text{ msec}$
- Slice thickness: $\leq 4 \text{ mm}$, no gap. Imaging planes should match or be similar to those used for T2W and DCE
- FOV: 16-22 cm
- In plane dimension: $\leq 2.5 \text{ mm}$ phase and frequency

For ADC maps, if only two b-values can be acquired due to time or scanner constraints, it is recommended to use one low b-value set at 0-100 sec/mm^2 (preferably 50-100 sec/mm^2) and one intermediate b-value set at 800-1000 sec/mm^2 . The maximum b-value used to calculate ADC is recommended to be $\leq 1,000 \text{ sec}/\text{mm}^2$ to avoid diffusion kurtosis effect that have been described at higher b-values. Nonetheless, a high b-value ($\geq 1,400 \text{ sec}/\text{mm}^2$) image set is also mandatory and preferably should be obtained from a separate acquisition or calculated from the low and intermediate b-value images. Additional b-values between 100 and 1000 may provide more accurate ADC calculations and estimations of calculated high b-value images ($>1400 \text{ sec}/\text{mm}^2$).

2. PI-RADS Assessment of DWI

Signal intensity in a lesion should be visually compared to the average signal of “normal” prostate tissue in the histologic zone in which it is located.

Score	Peripheral Zone (PZ) or Transition Zone (TZ)
1	No abnormality (i.e., normal) on ADC and high b-value DWI
2	Linear/wedge shaped hypointense on ADC and/or linear/wedge shaped hyperintense on high b-value DWI
3	Focal (discrete and different from the background) hypointense on ADC and/or focal hyperintense on high b-value DWI; may be markedly hypointense on ADC or markedly hyperintense on high b-value DWI, but not both.
4	Focal markedly hypointense on ADC and markedly hyperintense on high b-value DWI; <1.5cm in greatest dimension
5	Same as 4 but ≥1.5cm in greatest dimension or definite extraprostatic extension/invasive behavior

3. Caveats for DWI

- Findings on DWI should always be correlated with T2W, T1W, and DCE.
- Due to technical issues, units of signal intensity have not been standardized across different MRI scanners and are not analogous to Hounsfield units of density on CT. As a result, there are no standardized “prostate windows” that are applicable to images obtained from all MRI scanners. Clinically significant cancers have restricted/impeded diffusion and should appear as hypointense on the ADC map. It is strongly recommended that ADC maps from a particular scanner are set to portray clinically significant prostate cancers so that they appear markedly hypointense on ADC maps, and they should be consistently viewed with the same contrast (window width and level) settings. Guidance from radiologists who have experience with a particular vendor or scanner may be helpful.
- Color-coded maps of ADC may assist in standardization of viewing and assessing images from a particular scanner or vendor, but they will not obviate the concerns with reproducibility of quantitative ADC values.
- Benign findings and some normal anatomy (e.g. calculi and other calcifications, areas of fibrosis or dense fibromuscular stroma, and some blood products, usually from prior biopsies) may exhibit no or minimal signal on both T2W and ADC because there is insufficient signal. However, in contrast to clinically significant prostate cancers, these entities will also be markedly hypointense on all DWI images.
- Some BPH nodules in the TZ are not clearly encapsulated, and they may exhibit hypointensity on ADC maps and hyperintensity on high b-value DWI. Although morphologic features may assist assessment in some cases, this is currently a recognized limitation of mpMRI diagnosis.

- An encapsulated, circumscribed, round nodule in the PZ or CZ is likely an extruded BPH nodule, even if it is hypointense on ADC. PI-RADS Assessment Category for this finding should be category 2.
- The term “markedly” in category 4 is defined as a more pronounced signal change than any other focus in the same zone.

C. Dynamic Contrast-Enhanced (DCE) MRI

DCE MRI, is defined as the acquisition of rapid T1W gradient echo scans before, during and after the intravenous administration of a low molecular weight gadolinium-based contrast agent (GBCA). As with many other malignancies following bolus injection of a GBCA, prostate cancers often demonstrate early enhancement compared to normal tissue. However, the actual kinetics of prostate cancer enhancement are quite variable and heterogeneous. Some malignant tumors demonstrate early washout, while others retain contrast longer. Furthermore, enhancement alone is not definitive for clinically significant prostate cancer, and absence of early enhancement does not exclude the possibility.

DCE may help to detect some small significant cancers. The DCE data should always be closely inspected for focal early enhancement. If found, then the corresponding T2W and DWI images should be carefully interrogated for a corresponding abnormality. At present, the added value DCE is not firmly established, and most published data show that the added value of DCE over and above the combination of T2W and DWI is modest. Thus, although DCE is an essential component of the mpMRI prostate examination, its role in determination of PI-RADS v2.1 Assessment Category is secondary to T2W and DWI.

DCE is positive when there is enhancement that is focal, earlier or contemporaneous with enhancement of adjacent normal prostatic tissues, and usually corresponds to a suspicious finding on T2W and/or DWI. Positive enhancement in a lesion usually occurs within 10 seconds of the appearance of the injected GBCA in the femoral arteries (depending on temporal resolution used to acquire the images, injection rate, cardiac output, and other factors).

The most widely available method of analyzing DCE is direct visual assessment of the individual DCE time-points at each slice location by either manually scrolling or using cine mode. Visual assessment of enhancement may be improved with fat suppression or subtraction techniques (especially in the presence of blood products that are hyperintense on pre-contrast enhanced T1W). Visual assessment of enhancement may also be assisted with a parametric map which color-codes enhancement features within a voxel (e.g. slope and peak). However, any suspicious finding on subtracted images or a parametric map should always be confirmed on the source images.

Considerable effort has gone into “curve typing” (i.e. plotting the kinetics of a lesion as a function of signal vs. time). However, there is great heterogeneity in enhancement characteristics of prostate cancers, and at present there is little evidence in the literature to support the use of specific curve types. Another approach is the use of compartmental pharmacokinetic modeling, which incorporates contrast media concentration rather than raw signal intensity and an arterial input function to calculate time constants for the rate of contrast agent wash-in (Ktrans) and wash-out (kep). Commercial software programs are available that produce “maps” of Ktrans and kep and may improve lesion conspicuity. Although pharmacokinetic (PK) analysis may provide valuable insights into tumor behavior and biomarker measurements for drug development, the PI-RADS Steering

Committee believes there is currently insufficient peer reviewed published data or expert consensus to support routine adoption of this method of analysis for clinical use.

Thus, for PI-RADS™ v2.1, a “positive” DCE MRI lesion is one where the enhancement is focal, earlier or contemporaneous with enhancement of adjacent normal prostatic tissues, and corresponds to a finding on T2W and/or DWI. In the TZ, BPH nodules frequently enhance early, but they usually exhibit a characteristic benign morphology (round shape, well circumscribed). A “negative” DCE MRI lesion is one that either does not enhance early compared to surrounding prostate or enhances diffusely so that the margins of the enhancing area do not correspond to a finding on T2W and/or DWI.

1. Technical Specifications

DCE is generally carried out for several minutes to assess the enhancement characteristics. In order to detect early enhancing lesions in comparison to background prostatic tissue, temporal resolution should be <15 seconds per acquisition in order to depict focal early enhancement. However, a more rapid temporal resolution may be selected if maintaining sufficient spatial resolution and overall image quality is guaranteed. Fat suppression and/or subtractions is recommended.

- While both 2D or 3D T1W gradient echo (GRE) sequences have been described in the literature, 3D T1W GRE is generally available using modern systems and is preferred.
- TR/TE: <100msec/ <5msec
- Slice thickness: 3mm, no gap. Imaging planes should be the same as those used for DWI and DCE
- FOV: encompass the entire prostate gland and seminal vesicles
- In plane dimension: ≤2mm X ≤2mm
- Temporal resolution: ≤15sec
- Total observation rate: ≥2min
- Dose: 0.1mmol/kg standard GBCA or equivalent high relativity GBCA
- Injection rate: 2-3cc/sec starting with continuous image data acquisition (should be the same for all exams)

2. PI-RADS Assessment for DCE

Score	Peripheral Zone (PZ) or Transition Zone (TZ)
(–)	no early or contemporaneous enhancement; or diffuse multifocal enhancement NOT corresponding to a focal finding on T2W and/or DWI or focal enhancement corresponding to a lesion demonstrating features of BPH on T2WI (including features of extruded BPH in the PZ)
(+)	focal, and; earlier than or contemporaneously with enhancement of adjacent normal prostatic tissues, and; corresponds to suspicious finding on T2W and/or DWI

Caveats for DCE

- DCE should always be interpreted with T2W and DWI; Focal enhancement in clinically significant cancer usually corresponds to focal findings on T2W and/or DWI.
- DCE may be helpful when evaluation of DWI in part or all of the prostate is technically compromised (i.e., Assessment Category X) and when prioritizing multiple lesions in the same patient (e.g., all other factors being equal, the largest DCE positive lesion may be considered the index lesion).
- Diffuse enhancement on DCE is usually attributed to inflammation (e.g. prostatitis). Although infiltrating cancers may also demonstrate diffuse enhancement, these are uncommon and usually demonstrate an abnormality on the corresponding T2W and/or DWI.
- There are instances where histologically sparse prostate cancers are intermixed with benign prostatic tissues. They may be occult on T2W and DWI, and anecdotally may occasionally be apparent only on DCE. However, these are usually lower grade tumors, and the enhancement might, in some cases, be due to concurrent prostatitis.

3. Commentary on bi-parametric MRI

Despite the limited role of DCE in determining the overall PI-RADS assessment category experience has shown that, in some instances, DCE may assist in detection of csPCa in both the PZ and TZ, and in clinical practice some have viewed DCE as a 'safety-net' or 'back-up' sequence, especially when DWI is degraded by artifacts or inadequate signal-to-noise ratio (SNR).

Given the limited role of DCE, there is growing interest in performing prostate MRI without DCE, a procedure termed "biparametric MRI" (bpMRI). A number of studies have reported data that supports the value of bpMRI for detection of csPCa in biopsy-naïve men and those with a prior negative biopsy.

The PI-RADS Steering Committee supports continued research concerning the performance of bpMRI in various clinical scenarios and acknowledges the potential benefits, including: (1) elimination of adverse events and gadolinium retention that have been associated with some gadolinium based contrast agents (GBCAs), (2) shortened examination times, and (3) reduced costs, possibly resulting in increased accessibility and utilization of MRI for biopsy-naïve men with suspected prostate cancer.

However, the PI-RADS Steering Committee also has concern. In some studies, DCE-MRI has been reported to improve the sensitivity of prostate mpMRI. Although most of the bpMRI studies are prospective, and they were performed using different methodologies at single institutions with only one or two readers. It is possible that the performance of bpMRI will be degraded in multi-institutional clinical trials with multiple readers, and while further research is required, at this time there may be an increase in the frequency of missed csPCa's if bpMRI were to receive widespread clinical adoption. Furthermore, as described above, DCE in practice has been a 'safety-net' or 'back-up' sequence, especially when either T2W or DWI is degraded by artifacts or inadequate signal-to-noise ratio (SNR), a situation which is not uncommon on some MRI scanners when performing prostate MRI without an endorectal coil. Thus, it is important to

perform further research, before DCE is deemed unnecessary for assessment of treatment naïve prostate patients. DCE remains essential in assessment for local recurrence following prior treatment, a setting in which current PI-RADS assessment criteria do not apply.

The PI-RADS Steering Committee encourages multicenter prospective studies, employing multiple readers, addressing relative biopsy yields of csPCa and indolent PCa of mpMRI directed biopsy prompted by both approaches, with TRUS-GB comparisons to see if the documented advantages of mpMRI directed biopsy are retained by bpMRI.

For now, the Committee suggests that bpMRI be reserved for select clinical indications and makes the following recommendations for when mpMRI is preferred over bpMRI usage:

1. mpMRI is still preferred in men where the balance between under-diagnosis and over-diagnosis favors the clinical priority not to miss any significant cancer. These patients include those with prior negative biopsies with unexplained raised PSA values, and those in active surveillance who are being evaluated for fast PSA doubling times or changing clinical/pathologic status.
2. For men who have previously undergone a bpMRI exam that did not show findings suspicious for csPCa, and who remain at persistent suspicion of harboring disease, the clinical priority for subsequent MRI scans is to not miss csPCa; thus, the preferred reimaging option is mpMRI.
3. Prior prostate interventions (TRUS/TURP/BPH therapy, radiotherapy, focal therapy or embolization) and drug/hormonal therapies [testosterone, 5-alpha reductase, etc.] that are known to change prostate morphology should be evaluated with mpMRI, at a suitable time after the surgical intervention, for disease detection and localization.
4. Biopsy-naïve men with strong family history, known genetic predispositions, elevated urinary genomic scores and higher than average risk calculator scores for csPCa, should have mpMRI.
5. Men with a hip implant or other consideration that can be expected to yield degraded DWI should have mpMRI.

Implications of bpMRI for PI-RADS Assessment Categories

When bpMRI is performed and DCE data are not obtained, TZ assessment remains unchanged. The PI-RADS assessment category for a finding in the PZ remains primarily based on the DWI score and the lesions that receive a score of 3 on DWI will not be upgraded. The proportion of men with PI-RADS assessment category 3 will likely increase and PI-RADS 4 will reduce, and in so doing change the likelihood of csPCa in these PI-RADS categories, which will require additional documentation and subsequently pathway modifications for both biopsy naïve and prior negative biopsy men.

SECTION V: STAGING

MRI is useful for determination of the T stage, either confined to the gland (\neg T₂ disease) or extending beyond the gland ($>$ T₃ disease).

The apex of the prostate should be carefully inspected. When cancer involves the external urethral sphincter, there is surgical risk of cutting the sphincter, resulting in compromise of urinary competence. Tumor in this region may also have implications for radiation therapy.

High spatial resolution T₂W imaging is required for accurate assessment of extraprostatic extension (EPE), which includes assessment of neurovascular bundle involvement and seminal vesicle invasion. These may be supplemented by high spatial resolution contrast-enhanced fat suppressed T₁W.

The features of seminal vesicle invasion include focal or diffuse low T₂W signal intensity and/or abnormal contrast enhancement within and/or along the seminal vesicle, restricted diffusion, obliteration of the angle between the base of the prostate and the seminal vesicle, and demonstration of direct tumor extension from the base of the prostate into and around the seminal vesicle.

Imaging features used to assess for EPE include asymmetry or invasion of the neurovascular bundles, a bulging prostatic contour, an irregular or spiculated margin, obliteration of the rectoprostatic angle, a tumor-capsule interface of greater than 1.0 cm, breach of the capsule with evidence of direct tumor extension or bladder wall invasion.

The next level of analysis is that of the pelvic and retroperitoneal lymph nodes. The detection of abnormal lymph nodes on MRI is currently limited to size, morphology and shape, and enhancement pattern. In general, lymph nodes over 8mm in short axis dimension are regarded as suspicious, although lymph nodes that harbor metastases are not always enlarged. Nodal groups that should be evaluated include: common femoral, obturator, external iliac, internal iliac, common iliac, pararectal, presacral, and paracaval, and para-aortic to the level of the aortic bifurcation.

Images should be assessed for the presence of bone metastases.

APPENDIX I

Report Templates

The following provides a template for reporting mp-MRI using PI-RADS. The goal is to improve communication between practitioners. Therefore, it is important to keep in mind that the PI-RADS v2.1 overall suspicion category only applies when using the PI-RADS interpretation system. It is recommended that the overall suspicion category be given for each lesion, whereas the individual pulse sequence level categories are optional but may be helpful when determining the overall suspicion category. The overall suspicion should be reported in every case, although one can provide additional information which may modulate the final impression (e.g., when a peripheral zone lesion may be high suspicion but still consistent with prostatitis in the setting of bacteriuria, urgency, dysuria, and perineal pain).

It is also recommended that whether or not structures are involved (e.g., neurovascular bundles or seminal vesicles) be explicitly described rather than just giving a description of the appearance. Explicit reporting of the presumed stage is recommended, but optional.

When available, it is recommended the date and value of serum PSA level and prior biopsy should be reported; this may not be available in every case. Finally, it is recommended that the “technique” statement explicitly describe that the technique is PI-RADS-compliant, although whether the individual components (e.g. b-value for DWI) are explicitly described is optional. Dates of prior examinations should also be listed.

The PI-RADS report template begins on the next page.

PI-RADS Report Template

INDICATION: (including the date and value of serum PSA level and any prior biopsy type- TRUS, FUSION, IN BORE, date and results), prior therapy (Radiation, Hormones)

TECHNIQUE: (state it is PI-RADS-compliant; explicit description of field strength, coils used, route and rate of IV contrast administration, and pulse sequence parameters is recommended)

COMPARISON:**FINDINGS:**

Size: L x W x H cm or V cubic cm (with inclusion of PSA density)

Quality

Hemorrhage:

Peripheral zone:

Transition zone:

Lesion (s) in rank order of severity (highest score- to lowest score, then by size)

#1:

Location: use PI-RADS SECTOR LABEL and IMAGE SERIES/NUMBER

Size:

T2:

DWI:

DCE:

Prostate margin: (no involvement, indeterminate, or definite extraprostatic extension)

Lesion overall PI-RADS category:

Extra-prostatic extension:

Neurovascular bundles: Distance from index lesion or any PI-RADS 4/5 lesion to NVB's

Seminal vesicles:

Lymph nodes

Other pelvic organs:

IMPRESSION:

Overall PI-RADS category

(listing of PI-RADS categories)

Here is an example to consider

PROSTATE MRI

HISTORY/INDICATION: elevated serum PSA 2 weeks prior: 12.1 ng/mL

TECHNIQUE: multiplanar, multisequence imaging of the pelvis in accordance with PI-RADS recommendations before and after intravenous administration of 10 mL gadobutrol in the left antecubital fossa at 2.0 ml/sec on a 3.0 T platform using a 16-channel external phased array coil. Dedicated three-plane 20 cm FOV FSE T2; axial diffusion weighted imaging with b-values 50, 400, and 800 s/mm² and calculated b=1400 s/mm² and ADC map; and axial 3D dynamic contrast-enhanced T1-weighted imaging with 10 sec temporal resolution were acquired using 3 mm slice thickness in addition to full-pelvis post-contrast T1-weighted imaging.

(continued on next page)

COMPARISON: None

FINDINGS:

Size: 4.0 x 4.0 x 5.0 L x W x H cm for 42 cubic cm, PSA density 0.29 ng/mL/mL

Quality: mild geometric distortion on diffusion-weighted imaging from rectal distention does not compromise diagnostic confidence

Hemorrhage: none

Peripheral zone: Slightly heterogeneous high signal. Focal finding as below.

Transition zone: Moderate heterogeneity consistent with prostatic hyperplasia. Focal finding as below.

Lesion #1:

Location: right midgland transition zone anterior (RM-TZa) on series 5 image 16, axial T2

Size: 1.1 x 0.7 cm

T2: homogeneous, moderately hypointense with extraprostatic extension, sequence category 5/5

DWI: focal markedly hyperintense on high b-value DWI and markedly hypointense on ADC with extraprostatic extension, sequence category 5/5

DCE: focal early enhancement, positive

Prostate margin: gross extraprostatic extension anteriorly

Lesion overall PI-RADS category: 5/5

Lesion #2:

Location: left apex peripheral zone posterolateral (LX-PZpl) on series 8 image 20, ADC map

Size: 0.8 x 0.6 cm

T2: circumscribed, homogeneous, moderately hypointense, sequence category 4/5

DWI: focal mildly hyperintense on high b-value DWI and moderately hypointense on ADC, sequence category 3/5

DCE: focal early enhancement, positive

Prostate margin: does not abut the prostate margin

Lesion overall PI-RADS category: 4/5

Neurovascular bundles: Not involved, approximately 0.8 cm from lesion #2

Seminal vesicles: not involved

Lymph nodes: no lymphadenopathy

Bones: no osseous metastases suggested

Other pelvic organs: normal

IMPRESSION:

1. Very high suspicion right transition zone lesion with extraprostatic extension, MRI putative stage T3a (PI-RADS 5)
 2. High suspicion lesion left peripheral zone lesion without extraprostatic extension (PI-RADS 4)
- (continued on next page)*

Overall PI-RADS category 5

PI-RADS[®] v2.1 Assessment Categories

PI-RADS 1 – Very low (clinically significant cancer is highly unlikely to be present)

PI-RADS 2 – Low (clinically significant cancer is unlikely to be present)

PI-RADS 3 – Intermediate (the presence of clinically significant cancer is equivocal)

PI-RADS 4 – High (clinically significant cancer is likely to be present)

PI-RADS 5 – Very high (clinically significant cancer is highly likely to be present)

APPENDIX II

Sector Map

The segmentation model used in PI-RADS v2.1 employs 41 sectors/regions: 38 for the prostate, two for the seminal vesicles and one for the external urethral sphincter.

The prostate is divided into right/left on axial sections by a vertical line drawn through the center (indicated by the prostatic urethra), and into anterior/posterior by a horizontal line through the middle of the gland.

The right and left peripheral zones (PZ) at prostate base, mid gland, and apex are each subdivided into three sections: anterior (a), medial posterior (mp), and lateral posterior (lp).

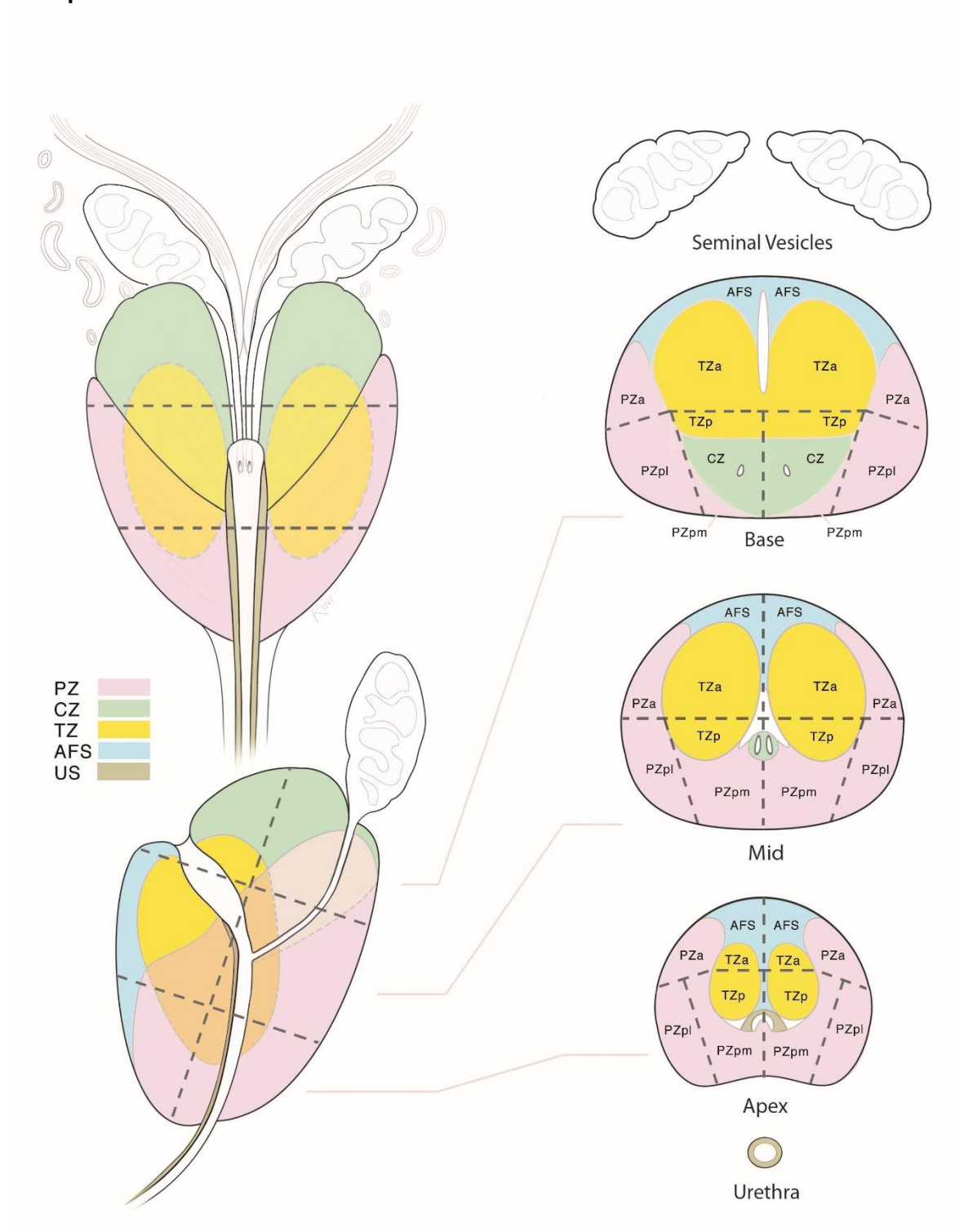
The right and left transition zones (TZ) at prostate base, mid gland, and apex are each subdivided into two sections: anterior (a) and posterior (p)

The anterior fibromuscular stroma (AS) is divided into right/left at the prostate base, mid gland, and apex. The seminal vesicles (SV) are divided into right/left.

The sector map illustrates an idealized “normal prostate”. In patients and their corresponding MRI images, many prostates have components that are enlarged or atrophied, and the PZ may be obscured by an enlarged TZ. In such instances, in addition to the written report, a sector map which clearly indicates the location of the findings will be especially useful for localization.

The PI-RADS Sector Map begins on the next page.

Sector Map



APPENDIX III

Lexicon

ABNORMALITY

Focal abnormality	Localized at a focus, central point or locus
Focus	Localized finding distinct from neighboring tissues, not a three-dimensional space occupying structure
Index Lesion	Lesion identified on MRI with the highest PIRADS Assessment Category. If the highest PIRADS Assessment Category is assigned to two or more lesions, the index lesion should be one that shows EPE or is largest. Also known as dominant lesion
Lesion	A localized pathological or traumatic structural change, damage, deformity, or discontinuity of tissue, organ, or body part
Mass	A three-dimensional space occupying structure resulting from an accumulation of neoplastic cells, inflammatory cells, or cystic changes
Nodule	A small lump, swelling or collection of tissue
Non-focal abnormality	Not localized to a single focus
Diffuse	Widely spread; not localized or confined; distributed over multiple areas, may or may not extend in contiguity, does not conform to anatomical boundaries
Multifocal	Multiple foci distinct from neighboring tissues
Regional	Conforming to prostate sector, sextant, zone, or lobe; abnormal signal other than a mass involving a large volume of prostatic tissue

SHAPE

Round	The shape of a circle or sphere
Oval	The shape of either an oval or an ellipse
Lenticular	Having the shape of a double-convex lens, crescentic
Lobulated	Composed of lobules with undulating contour
Water-drop-shaped Tear-shaped	Having the shape of a tear or drop of water; it differs from an oval because one end is clearly larger than the other
Wedge-shaped	Having the shape of a wedge, pie, or V-shaped
Linear	In a line or band-like shape
Irregular	Lacking symmetry or evenness

MARGINS

Circumscribed	Well defined
Non-circumscribed	Ill-defined
Indistinct	Blurred
Obscured	Not clearly seen or easily distinguished
Irregular	Uneven
Spiculated	Radiating lines extending from the margin of a mass
Encapsulated	Bounded by a distinct, uniform, smooth low-signal line (BPH nodule); completely encapsulated nodule is entirely surrounded by a smooth low-signal line in at least two imaging planes (“typical nodule”); almost completely or incompletely encapsulated nodule is not entirely surrounded by a smooth low-signal line (“atypical nodule”)
Erased charcoal sign	Blurred margins as if smudged, smeared with a finger; refers to appearance of a homogeneously T2 low-signal lesion in the transition zone of the prostate with indistinct margins (prostate cancer)

MR IMAGING SIGNAL CHARACTERISTICS

Hyperintense	Having higher signal intensity (more intense, brighter) on MRI than background prostate tissue or reference tissue/structure
T2 Hyperintensity	Having higher signal intensity (more intense, brighter) on T2- weighted imaging
Isointense	Having the same intensity as a reference tissue/structure to which it is compared; intensity at MRI that is identical or nearly identical to that of background prostate
Hypointense	Having less intensity (darker) than background prostate tissue or reference tissue/structure
Markedly hypointense	Signal intensity lower than expected for normal or abnormal tissue of the reference type, e.g., when involved with calcification or blood or gas
T2 hypointensity	Having lower signal intensity (less intense, darker) on T2-weighted imaging
ADCHypointense	Having lower intensity (darker) than a reference background tissue on ADC map
Organized chaos	Heterogeneous T2 signal-intensity in transition zone with circumscribed margins, encapsulated (BPH nodule)

Restricted diffusion	Limited, primarily by cell membrane boundaries, random Brownian motion of water molecules within the voxel; having higher signal intensity than peripheral zone or transition zone prostate on DW images acquired or calculated at b values $>1400 \text{ sec/mm}^2$ accompanied by low signal intensity on the corresponding ADC map. Synonymous with "impeded" diffusion
Diffusion-weighted hyperintensity	Having higher signal intensity, not attributable to T2 shine-through, than background prostate on DW images
Apparent Diffusion Coefficient (ADC)	A measure of the degree of motion of water molecules in tissues. It is determined by calculating the signal loss in data obtained with different b-values and is expressed in units of mm^2/sec or $\mu\text{m}^2/\text{sec}$
ADC Map	A display of ADC values for each voxel in an image
ADC Hyperintense	Having higher signal intensity (more intense, brighter) than background tissue on ADC map
ADC Isointense	Intensity that is identical or nearly identical to that of background tissue on ADC map
ADC Hypointense	Having lower signal intensity (darker) than a reference background tissue on ADC map
b-value	A measure of the strength and duration of the diffusion gradients that determines the sensitivity of a DWI sequence to diffusion
Dynamic contrast enhanced (DCE) Wash-in	Early arterial phase of enhancement; a period of time to allow contrast agent to arrive in the tissue
DCE Wash-out	Later venous phase, de-enhancement, reduction of signal following enhancement; a period of time to allow contrast agent to clear the tissue
Pharmacodynamic analysis PD curves	Method of quantifying tissue contrast media concentration changes to calculate time constants for the rate of wash-in and wash-out
Time vs. signal intensity curve	Graph plotting tissue intensity change (y axis) over time (x axis); enhancement kinetic curve is
Enhancement kinetic curve	a graphical representation of tissue enhancement where signal intensity of tissue is plotted as a function of time

ENHANCEMENT PATTERNS

Early phase wash-in	Signal intensity characteristic early after contrast agent administration; wash-in phase corresponding to contrast arrival in the prostate
Delayed phase	Signal intensity characteristic following its initial (early) rise after contrast material administration
Persistent delayed phase – Type 1 curve	Continued increase of signal intensity over time
Plateau delayed phase – Type 2 curve	Signal intensity does not change over time after its initial rise, flat; plateau refers to signal that varies <10% from the peak signal over the duration of the DCE MRI
Washout delayed phase – Type 3 curve	Signal intensity decreases after its highest point after its initial rise
Positive DCE	Focal, AND earlier than OR contemporaneous with adjacent normal prostatic tissues enhancement AND corresponding to a peripheral zone or transition zone lesion on T2 and/or DWI
Negative DCE	Lack of early or contemporaneous with adjacent normal prostatic tissues enhancement Diffuse multifocal enhancement NOT corresponding to a focal lesion on T2 and/or DWI Focal enhancement corresponding to a BPH lesion

ANATOMICAL TERMS

Prostate: Regional Parts	The prostate is divided from superior to inferior into three regional parts: the base, the midgland, and the apex
Base of prostate	The upper 1/3 of the prostate just below the urinary bladder
Mid prostate	The middle 1/3 of the prostate that includes verumontanum in the mid prostatic urethra; midgland
Apex of prostate	The lower 1/3 of the prostate
Peripheral zone	Covers the outer posterior, lateral, and apex regions of the prostate; makes up most of the apex of the prostate
Transition zone	Tissue along the proximal prostatic urethra that enlarges with ageing (BPH). It is separated from the peripheral zone by a “surgical capsule” (or “pseudocapsule”) delineated as a low signal line on T2 weighted MRI

Central zone	Tissue surrounding the ejaculatory ducts posterior and superior, from the base of the prostate to the verumontanum; it has the shape of an inverted cone with its base oriented towards the base of the gland; contains more stroma than glandular tissue
Anterior fibromuscular stroma	Located anteriorly and contains smooth muscle, which mixes with periurethral muscle fibers at the bladder neck; contains no glandular tissue
Prostate: Sectors	Anatomical regions defined for the purpose of prostate targeting during interventions, may include multiple constitutional and regional parts of the prostate. Thirty-eight sectors for standardized MRI prostate localization reporting are identified, with addition of seminal vesicles and membranous urethra. Each traditional prostate sextant is sub-divided into six sectors, to include: the anterior fibromuscular stroma, the transition zone anterior and posterior sectors, the peripheral zone anterior, lateral, and medial sectors. The anterior and posterior sectors are defined by a line bisecting the prostate into the anterior and posterior halves. See Sector Map Diagram
Prostate “capsule”	Histologically, there is no distinct capsule that surrounds the prostate, however historically the “capsule” has been defined as an outer band of the prostatic fibromuscular stroma blending with endopelvic fascia that may be visible on imaging as a distinct thin layer of tissue surrounding or partially surrounding the peripheral zone
Prostate pseudocapsule	Imaging appearance of a thin “capsule” around transition zone when no true capsule is present at histological evaluation. The junction of the transition and peripheral zones marked by a visible hypointense linear boundary, which is often referred to as the prostate “pseudocapsule” capsule” or “surgical
Seminal vesicle	One of the two paired glands in the male genitourinary system, posterior to the bladder and superior to the prostate gland, that produces fructose-rich seminal fluid which is a component of semen. These glands join the ipsilateral ductus (vas) deferens to form the ejaculatory duct at the base of the prostate
Neurovascular bundle of prostate (NVB)	Nerve fibers from the lumbar sympathetic chain extend inferiorly to the pelvis along the iliac arteries and intermix with parasympathetic nerve fibers branching off S2 to S4. The mixed nerve bundles run posterior to the bladder, seminal vesicles, and prostate as the “pelvic plexus”. The cavernous nerve arises from the pelvic plexus and runs along the posterolateral aspect of the prostate on each side. Arterial and venous vessels accompany the cavernous nerve, and together these structures form the neurovascular bundles which are best visualized on MR imaging at 5 and 7 o’clock position. At the apex and the base of the prostate, the bundles send penetrating branches through the “capsule”, providing a potential route for extraprostatic tumor spread.

Right neurovascular bundle	Located at 7 o'clock postero-lateral position.
Left neurovascular bundle	Located at 5 o'clock postero-lateral position.
Vas deferens	The excretory duct of the testes that carries spermatozoa; it rises from the scrotum and joins the seminal vesicles to form the ejaculatory duct, which opens into the mid prostatic urethra at the level of the verumontanum.
Verumontanum	The verumontanum (urethral crest formed by an elevation of the mucous membrane and its subjacent tissue) is an elongated ridge on the posterior wall of the mid prostatic urethra at the site of ejaculatory ducts opening into the prostatic urethra
Neck of urinary bladder	The inferior portion of the urinary bladder which is formed as the walls of the bladder converge and become contiguous with the proximal urethra
Urethra: Prostatic	The proximal prostatic urethra extends from the bladder neck at the base of the prostate to verumontanum in the mid prostate. The distal prostatic urethra extends from the verumontanum to the membranous urethra and contains striated muscle of the urethral sphincter
Urethra: Membranous	The membranous segment of the urethra is located between the apex of the prostate and the bulb of the corpus spongiosum, extending through the urogenital diaphragm
External urethral sphincter	Surrounds the whole length of the membranous portion of the urethra and is enclosed in the fascia of the urogenital diaphragm
Periprostatic compartment	Space surrounding the prostate
Rectoprostatic compartment / Rectoprostatic angle	Space between the prostate and the rectum
Extraprostatic	Pertaining to an area outside the prostate
Prostate–seminal vesicle angle	The plane or space between the prostate base and the seminal vesicle, normally filled with fatty tissue and neurovascular bundle of prostate

STAGING TERMS

Abuts "capsule" of prostate	Tumor touches the "capsule"
Bulges "capsule" of prostate	Convex contour of the "capsule" Bulging prostatic contour over a suspicious lesion: Focal, spiculated (extraprostatic tumor) Broad-base of contact (at least 25% of tumor contact with the capsule) Tumor-capsule abutment of greater than 1cm Lenticular tumor at prostate apex extending along the urethra below the apex
Mass effect on surrounding tissue	Compression of the tissue around the mass, or displacement of adjacent tissues or structures, or obliteration of the tissue planes by an infiltrating mass
Invasion	Tumor extension across anatomical boundary; may relate to tumor extension within the gland, i.e. across regional parts of the prostate, or outside the gland, across the "capsule" (extracapsular extension of tumor, extraprostatic extension of tumor, extraglandular extension of tumor)
Invasion: "Capsule"	Tumor involvement of the "capsule" or extension across the "capsule" with indistinct, blurred or irregular margin
Extraprostatic extension EPE	Retraction of the capsule Breach of the capsule Direct tumor extension through the "capsule" Obliteration of the rectoprostatic angle
Invasion: Pseudocapsule	Tumor involvement of pseudocapsule with indistinct margin
Invasion: Anterior fibromuscular stroma	Tumor involvement of anterior fibromuscular stroma with indistinct margin
Invasion: Prostate–seminal vesicle angle	Tumor extends into the space between the prostate base and the seminal vesicle

Invasion: Seminal vesicle Seminal vesicle invasion SVI	Tumor extension into seminal vesicle There are 3 types: 1. Tumor extension along the ejaculatory ducts into the seminal vesicle above the base of the prostate; focal T2 hypointense signal within and/or along the seminal vesicle; enlargement and T2 hypointensity within the lumen of seminal vesicle; Restricted diffusion within the lumen of seminal vesicle; Enhancement along or within the lumen of seminal vesicle; Obliteration of the prostate-seminal vesicle angle 2. Direct extra-glandular tumor extension from the base of the prostate into and around the seminal vesicle 3. Metachronous tumor deposit –separate focal T2 hypointense signal, enhancing mass in distal seminal vesicle
Invasion: Neck of urinary bladder	Tumor extension along the prostatic urethra to involve the bladder neck
Invasion: Membranous urethra	Tumor extension along the prostatic urethra to involve the membranous urethra
Invasion: Periprostatic, extraprostatic	Tumor extension outside the prostate
Invasion: Neurovascular bundle of prostate	Tumor extension into the neurovascular bundle of the prostate Asymmetry, enlargement or direct tumor involvement of the neurovascular bundles Assess the recto-prostatic angles (right and left): 1. Asymmetry – abnormal one is either obliterated or flattened 2. Fat in the angle – infiltrated (individual elements cannot be identified or separated) Clean (individual elements are visible) 3. Direct tumor extension
Invasion: External urethral sphincter	Tumor extension into the external urethral sphincter Loss of the normal low signal of the sphincter, discontinuity of the circular contour of the sphincter

MRI CHARACTERISTICS OF ADDITIONAL PATHOLOGIC STATES

BPH nodule	A round/oval mass with a well-defined T2 hypointense margin in at least two planes of imaging; encapsulated mass or “organized chaos” found in the transition zone or extruded from the transition zone into the peripheral zone
Hypertrophy of median lobe of prostate	Increase in the volume of the median lobe of the prostate with mass-effect or protrusion into the bladder and stretching the urethra
Cyst	A circumscribed T2 hyperintense fluid containing sac-like structure
Hematoma - Hemorrhage	T1 hyperintense collection or focus
Calcification	Focus of markedly hypointense signal on all MRI sequences

APPENDIX IV

SAMPLE PROTOCOLS (this section is under construction)

APPENDIX V

Atlas

(Available at www.acr.org/Clinical-Resources/Reporting-and-Data-Systems/PI-RADS)

REFERENCES

Introduction

1. Thornbury JR, Ornstein DK, Choyke PL, Langlotz CP, Weinreb JC. Prostate Cancer: What is the future for imaging? *Am J Roentgenology* 2001;176:17-22.
2. Dickinson L, Ahmed HU, Allen C, Barentsz JO, Carey B, Futterer JJ, et al. Magnetic resonance imaging for the detection, localisation, and characterisation of prostate cancer: recommendations from a European consensus meeting. *European Urology*.2011;4:477-94.
3. Eberhardt SC, Carter S, Casalino DD, Merrick G, Frank SJ, et al. ACR Appropriateness Criteria® for Prostate Cancer — pretreatment detection, staging and surveillance. *J Am Coll Radiol*2013;10(2); 83-92
4. Barentsz JO, Richenberg J, Clements R, Choyke P, Verma S, Villeirs G, et al. ESUR prostate MR guidelines 2012. *European Radiol* 2012;4:746-57.
5. Moore CM, Kasivisvanathan V, Eggner S, Emberton M, Futterer JJ, et al. Standards of reporting for MRI-targeted biopsy studies (START) of the prostate: recommendations from an international working group. *European Urology* 2013;64:544-552
6. Rosenkrantz AB, Kim S, Lim RP, Hindman N, Deng F-M, et al. Prostate cancer localization using multiparametric MR imaging: comparison of Prostate Imaging Reporting and Data System (PI-RADS) and Likert Scales. *Radiology* 2013;269:482-492
7. de Rooij M, Hamoen EHJ, Futterer JJ, Barentsz JO, Rovers MM. Accuracy of multiparametric MRI for prostate cancer detection: a meta-analysis. *Am J Roentgenology*2014;202:343-351
8. Arumainayagam N, Ahmed HU, Moore CM, Freeman A, Allen C, et al. Multiparametric MR imaging for detection of clinically significant prostate cancer: a validation cohort study with transperineal template prostate mapping as the reference standard. *Radiology* 2013;268:761-769
9. Dickinson L, Ahmed HU, allen C, Barentsz JO, Carey B, et al. Scoring systems used for the interpretation and reporting of multiparametric MRI for prostate cancer detection, localization and characterization: could standardization lead to improved utilization of imaging within the diagnostic pathway? *J Magn Reson imaging* 2013;37:48-58
10. Cornelis F, Rigou G, Le Bras Y, Coutouly X, Hubrecht R, et al. Real-time contrast-enhanced transrectal US-guided prostate biopsy: diagnostic accuracy in men with previously negative biopsy results and positive MR imaging findings. *Radiology* 2013;269:159-166
11. Puech P, Rouviere O, renard-Penna R, Villers A, Devos P, et al. Prostate cancer diagnosis: multiparametric MR-targeted biopsy with cognitive and transrectal U-MR fusion guidance versus systemic biopsy-prospective multicenter study. *Radiology*2013;268;461-469
12. Pokorny MR, de Rooij M, Duncan E, Schroder FH, Parkinson R, et al. Prospective study of diagnostic accuracy comparing prostate cancer detection by transrectal ultrasound-guided biopsy versus magnetic resonance (MR) imaging with subsequent MR-guided biopsy in men without previous prostate biopsies. *European Urology* 2014;66:22-29

13. Hamoen EHJ, de Rooij M, Witjes JA, Barentsz J. Use of the Prostate Imaging Reporting and Data System (PI-RADS) for prostate cancer detection with multiparametric magnetic resonance imaging: a diagnostic meta-analysis. *European Urology* 2015;67:1112-1121
14. Renard-Penna R, Rouviere O, Puech P, Borgogno C, Abbas L, Roy C, et al. Current practice and access to prostate MR imaging in France. *Diagnostic and interventional imaging*. 2016;97:1125-1129
15. Oberlin DT, Casalino DD, Miller FH, Meeks JJ. Dramatic increase in the utilization of multiparametric magnetic resonance imaging for detection and management of prostate cancer. *Abdom Radiol (NY)*. 2017;42:1255-1258
16. Gupta RT, Spilseth B, Froemming AT. How and why a generation of radiologists must be trained to accurately interpret prostate mpMRI. *Abdom Radiol (NY)*. 2016;41:803-804
17. Weinreb JC, Barentsz JO, Choyke PL, Cornud F, Haider MA, Macura KJ, et al. PI-RADS Prostate Imaging - Reporting and Data System: 2015, Version 2. *European urology*. 2016;69:16-40
18. Spilseth BD GS, Patel NU, Taneja SS, Margolis DJ, Rosenkrantz AB. A Comparison of Radiologists' and Urologists' Opinions Regarding Prostate MRI Reporting: Results from a Survey of Specialty Societies. *American Journal of Roentgenology*. 2018;210:101-107
19. Purysko AS, Bittencourt LK, Bullen JA, Mostardeiro TR, Herts BR, Klein EA. Accuracy and Interobserver Agreement for Prostate Imaging Reporting and Data System, Version 2, for the Characterization of Lesions Identified on Multiparametric MRI of the Prostate. *AJR American journal of roentgenology*. 2017;209:339-349
20. Seo JW, Shin SJ, Taik Oh Y, Jung DC, Cho NH, Choi YD, et al. PI-RADS Version 2: Detection of Clinically Significant Cancer in Patients With Biopsy Gleason Score 6 Prostate Cancer. *AJR American journal of roentgenology*. 2017;209(1):W1-w9
21. Mehralivand S, Bednarova S, Shih JH, Mertan FV, Gaur S, Merino MJ, et al. Prospective Evaluation of Prostate Imaging Reporting and Data System, Version 2 Using the International Society of Urological Pathology Prostate Cancer Grade Group System. *J Urol*. 2017;198:583-590
22. Woo S, Suh CH, Kim SY, Cho JY, Kim SH. Diagnostic Performance of Prostate Imaging Reporting and Data System Version 2 for Detection of Prostate Cancer: A Systematic Review and Diagnostic Meta-analysis. *European urology*. 2017;72:177-188
23. Padhani AR, Weinreb J, Rosenkrantz AB, Villeirs G, Turkbey B, Barentsz J. Prostate Imaging-Reporting and Data System Steering Committee: PI-RADS v2 Status Update and Future Directions. *European urology*. 2019;75:385-396
24. Greer MD, Shih JH, Lay N, Barrett T, Kayat Bittencourt L, Borofsky S, et al. Validation of the Dominant Sequence Paradigm and Role of Dynamic Contrast-enhanced Imaging in PI-RADS Version 2. *Radiology*. 2017;285:859-869
25. Rosenkrantz AB, Babb JS, Taneja SS, Ream JM. Proposed Adjustments to PI-RADS Version 2 Decision Rules: Impact on Prostate Cancer Detection. *Radiology*. 2017;283:119-129
26. Greer MD, Brown AM, Shih JH, Summers RM, Marko J, Law YM, et al. Accuracy and agreement of PIRADSv2 for prostate cancer mpMRI: A multireader study. *J Magn Reson Imaging*. 2017;45:579-585

27. Rosenkrantz AB, Ginocchio LA, Cornfeld D, Froemming AT, Gupta RT, Turkbey B, et al. Interobserver Reproducibility of the PI-RADS Version 2 Lexicon: A Multicenter Study of Six Experienced Prostate Radiologists. *Radiology*. 2016;280:793-804
28. Rosenkrantz AB, Oto A, Turkbey B, Westphalen AC. Prostate Imaging Reporting and Data System (PI-RADS), Version 2: A Critical Look. *AJR American journal of roentgenology*. 2016;206:1179-1183

SECTION I: CLINICAL CONSIDERATIONS AND TECHNICAL SPECIFICATIONS

1. Wagner M, Rief M, Busch, Scheuring C, Taupitz M, et al. Effect of butylscopolamine on image quality in MRI of the prostate. *Clin radiol* 2012;65:460-465
2. Rosenkrantz AB, Kopec M, Kong X, Melamed J, Dakwar G, Babb JS, et al. Prostate cancer vs. post-biopsy hemorrhage: diagnosis with T2- and diffusion-weighted imaging. *J Magn Reson Imaging* 2010 Jun;31(6):1387-94.
3. Rosenkrantz AB, Mussi TC, Hindman N, Lim RP, Knong MX, et al. Impact of delay after biopsy and post-biopsy haemorrhage on prostate cancer tumor detection using multi-parametric MRI: a multi-reader study. *Clin Radiol* 2012;67:83-90
4. Tamada T, Sone T, Jo Y, Yamamoto A, Yamashita T, Egashira N, et al. Prostate cancer: relationships between postbiopsy hemorrhage and tumor detectability at MR diagnosis. *Radiology* 2008;248:531-539
5. Barrett T, Vargas HA, Akin O, Goldman DA, Hricak H. Value of the hemorrhage exclusion sign on T1-weighted prostate MR images for the detection of prostate cancer. *Radiology* 2012;263:751-757
6. Park KK, Lee SH, Lim BJ, Kim JH, Chung BH. The effects of the period between biopsy and diffusion-weighted magnetic resonance imaging on cancer staging in localized prostate cancer. *BJU Int* 2010;106:1148-1151
7. Medved M, Sammet S, Yousuf A, Oto A. MR imaging of the prostate and adjacent anatomic structures before, during, and after ejaculation: qualitative and quantitative evaluation. *Radiology* 2014;271(2):452-60.
8. Rouviere O, Hartman RP, Lyonnet D. Prostate MR imaging at high-field strength: evolution or revolution? *European Radiol* 2006;16(2):276-84.
9. Johnston R, Wong L-M, Warren A, Shah N, Neal D. The role of 1.5T Tesla magnetic resonance imaging in staging prostate cancer. *ANZ J Surg* 2013(83);234-238
10. Kim BS, Kim TH, Kwon TG, Yoo ES. Comparison of pelvic phased-array versus endorectal coil magnetic resonance imaging at 3 Tesla for local staging of prostate cancer. *Yonsei Med J* 2012;53(3):550-6.
11. Turkbey B, Merinio MJ, Gallardo EC, Shah V, Aras O, et al. Comparison of endorectal and nonendorectal coil T2W and diffusion-weighted MRI at 3 Tesla for localizing prostate cancer: comparison with whole-mount histopathology. *J Magn Reson Imaging* 2014;39:1443-1448
12. Haider MA, Krieger A, Elliot C, Da Rosa MR, Milot L. Prostate imaging: evaluation of reusable two-channel endorectal receiver coil for MR imaging at 1.5T. *Radiology* 2014;270:556-565

13. Leake JL, Hardman R, Vijayanadh O, Thompson I, Shanbhogue A, et al. prostate MRI: access to the current practice of prostate MRI in the United States. *J Am Coll Radiol* 2014;11:156-160
14. Rosen Y, Bloch N, Lenkinski RE, Greenman RL, Marquis RP, Rofsky NM. 3T MR of the prostate: reducing susceptibility gradients by inflating the endorectal coil with barium sulfate suspension. *Magn Reson Med* 2007;57:898-904
15. Roethke MC, Kuru TH, Schultze S, Tichy D, Kopp-Schneider A, Fenchel M, et al. Evaluation of the ESUR PI-RADS scoring system for multiparametric MRI of the prostate with targeted MR/TRUS fusion-guided biopsy at 3.0 Tesla. *European Radiol* 2014 Feb;24(2):344-52.
16. Niaf E, Lartzien C, Bratan F, Roche L, Babilloud M, et al. Prostate focal peripheral zone lesions; characterization at multiparametric MR imaging-influence of computer-aided diagnosis system. *Radiology* 2014;271:761-769
17. Hambrock T, Vos PC, Hulsbergen-van de Kaa CA, Barentsz JO, Huisman HJ. Prostate cancer: computer-aided diagnosis with multiparametric 3-T MR imaging- effect on observer performance. *Radiology* 2013;266:521-530
18. Rosenkrantz AB, Padhani AR, Chenevert TL, Koh DM, De Keyzer F, Taouli B, et al. Body diffusion kurtosis imaging: Basic principles, applications, and considerations for clinical practice. *J Magn Reson Imaging*. 2015;42:1190-1202
19. Ream JM, Doshi AM, Dunst D, Parikh N, Kong MX, Babb JS, et al. Dynamic contrast-enhanced MRI of the prostate: An intraindividual assessment of the effect of temporal resolution on qualitative detection and quantitative analysis of histopathologically proven prostate cancer. *J Magn Reson Imaging*. 2017;45:1464-1475
20. Othman AE, Falkner F, Weiss J, Kruck S, Grimm R, Martirosian P, et al. Effect of Temporal Resolution on Diagnostic Performance of Dynamic Contrast-Enhanced Magnetic Resonance Imaging of the Prostate. *Investigative radiology*. 2016;51:290-296
21. Boesen L, Nørgaard N, Løgager V, Balslev I, Bisbjerg R, Thstrup KC, Winther MD, Jakobsen H, Thomsen HS. Assessment of the Diagnostic Accuracy of Biparametric Magnetic Resonance Imaging for Prostate Cancer in Biopsy-Naive Men: The Biparametric MRI for Detection of Prostate Cancer (BIDOC) Study. *JAMA Netw Open*. 2018;1:e180219
22. Jambor I, Bostrom PJ, Taimen P, Syvanen K, Kahkonen E, Kallajoki M, et al. Novel biparametric MRI and targeted biopsy improves risk stratification in men with a clinical suspicion of prostate cancer (IMPROD Trial). *J Magn Reson Imaging*. 2017;46:1089-1095
23. Cuocolo R, Stanzione A, Rusconi G, Petretta M, Ponsiglione A, Fusco F, et al. PSA-density does not improve bi-parametric prostate MR detection of prostate cancer in a biopsy naive patient population. *European journal of radiology*. 2018;104:64-70
24. Weiss J, Martirosian P, Notohamiprodjo M, Kaufmann S, Othman AE, Grosse U, et al. Implementation of a 5-Minute Magnetic Resonance Imaging Screening Protocol for Prostate Cancer in Men With Elevated Prostate-Specific Antigen Before Biopsy. *Investigative radiology*. 2018;53:186-190

25. Barth BK, De Visschere PJL, Cornelius A, Nicolau C, Vargas HA, Eberli D, et al. Detection of Clinically Significant Prostate Cancer: Short Dual-Pulse Sequence versus Standard Multiparametric MR Imaging-A Multireader Study. *Radiology*. 2017;284:725-736
26. Krishna S, McInnes M, Lim C, Lim R, Hakim SW, Flood TA, et al. Comparison of Prostate Imaging Reporting and Data System versions 1 and 2 for the Detection of Peripheral Zone Gleason Score 3 + 4 = 7 Cancers. *AJR American journal of roentgenology*. 2017;209:W365-w73
27. Kuhl CK, Bruhn R, Kramer N, Nebelung S, Heidenreich A, Schrading S. Abbreviated Biparametric Prostate MR Imaging in Men with Elevated Prostate-specific Antigen. *Radiology*. 2017;285:493-505

SECTION II: NORMAL ANATOMY AND BENIGN FINDINGS

1. McNeal JE. The Zonal anatomy of the prostate. *The Prostate* 1981;2:35-49
2. McNeal JE. Normal histology of the prostate. *Am J SurgPathol* 1988;12:619-33
3. Villers A, Lemaitre L, Haffner J, Puech P. Current status of MRI for the diagnosis, staging and prognosis of prostate cancer: implications for focal therapy and active surveillance. *Curr Opin Urol* 2009;19:274-82
4. Vargas HA, Akin O, Franiel T, Goldman DA, Udo K, et al. Normal central zone of the prostate and central zone involvement by prostate cancer: clinical and MR imaging implications. *Radiology* 2012;262:894-902
5. Shebel HM, Farg HM, Kolokythas O, El-Diasty T. Cysts of the lower male genitourinary tract: embryologic and anatomic considerations and differential diagnosis. *Radiographics* 2013Jul-Aug;33(4):1125-43.
6. Krieger JN, Lee SWH, Jeon J, Cheah PY, Liong ML, et al. Epidemiology of prostatitis. *Int J Antimicrob Agents* 2008;31 (Suppl 1): 85-90
7. Nagel NNA, Schouten MG, Hambrock T, Litjens GJS, Hoeks CMA, et al. Differentiation of prostatitis and prostate cancer by using diffusion-weighted MR imaging and MR-guided biopsy at 3T. *Radiology* 2013;267:164-172
8. Engelhard K, Hollenback HP, Deimiing M, Kerckel M, Riedi C. Combination of signal intensity measurements of lesions in the peripheral zone of prostate with MRI and serum PSA level for differentiating benign disease from prostate cancer. *Eur Radiol* 2000;10(12):1947-1953
9. Vargas HA, Akin O, Franiel T, Goldman DA, Udo K, Touijer KA, et al. Normal central zone of the prostate and central zone involvement by prostate cancer: clinical and MR imaging implications. *Radiology*. 2012;262:894-902
10. Turkbey B, Huang R, Vourganti S, Trivedi H, Bernardo M, Yan P, et al. Age-related changes in prostate zonal volumes as measured by high-resolution magnetic resonance imaging (MRI): a cross-sectional study in over 500 patients. *BJU international*. 2012;110:1642-1647
11. Chesnais AL, Niaf E, Bratan F, Mege-Lechevallier F, Roche S, Rabilloud M, et al. Differentiation of transitional zone prostate cancer from benign hyperplasia nodules: evaluation of discriminant criteria at multiparametric MRI. *Clinical radiology*. 2013;68:e323-330

12. Lee SJ, Oh YT, Jung DC, Cho NH, Choi YD, Park SY. Combined Analysis of Biparametric MRI and Prostate-Specific Antigen Density: Role in the Prebiopsy Diagnosis of Gleason Score 7 or Greater Prostate Cancer. *AJR American journal of roentgenology*. 2018;211:W166-w72
13. Mehralivand S, Shih JH, Rais-Bahrami S, Oto A, Bednarova S, Nix JW, et al. A Magnetic Resonance Imaging-Based Prediction Model for Prostate Biopsy Risk Stratification. *JAMA oncology*. 2018;4:678-685

SECTION III: ASSESSMENT AND REPORTING

1. Epstein JI, Walsh PC, Carmichael M, Brendler CB. Pathologic and clinical findings to predict tumor extent of nonpalpable (stage T1c) prostate cancer. *JAMA* 1994 Feb2;271(5):368-74.
2. Goto Y, Ohori M, Arakawa A, Kattan MW, Wheeler TM, Scardino PT. Distinguishing clinically important from unimportant prostate cancers before treatment: value of systematic biopsies. *J Urol* 1996 Sep;156(3):1059-63.
3. Harnden P, Naylor B, Shelley MD, Clements H, Coles B, Mason MD. The clinical management of patients with a small volume of prostatic cancer on biopsy: what are the risks of progression? A systematic review and meta-analysis. *Cancer* 2008 Mar1;112(5):971-81.
4. Wolters T, Roobol MJ, van Leeuwen PJ, van den Bergh RC, Hoedemaeker RF, van Leenders GJ, et al. A critical analysis of the tumor volume threshold for clinically insignificant prostate cancer using a data set of a randomized screening trial. *J Urol* 2011 Jan;185(1):121-5.
5. Vargas HA, Akin O, Shukla-Dave A, Zhang J, Zakian KL, et al. Performance characteristics of MR imaging in the evaluation of clinically low-risk prostate cancer: a prospective study. *Radiology* 2012; 265:478-487
6. Ren J, Yang Y, Zhang J, Xu J, Liu Y, Wei M, et al. T(2)-weighted combined with diffusion-weighted images for evaluating prostatic transition zone tumors at 3 Tesla. *Future Oncol* 2013Apr;9(4):585-93.
7. Delongchamps NB, Rouanne M, Flam T, Beuvon F, Liberatore M, Zerbib M, et al. Multiparametric magnetic resonance imaging for the detection and localization of prostate cancer: combination of T2-weighted, dynamic contrast-enhanced and diffusion-weighted imaging. *BJU international*. 2011 May;107(9):1411-8.
8. Turkbey B, Pinto PA, Mani H, Bernardo M, Pang Y, McKinney YL, et al. Prostate cancer: value of multiparametric MR imaging at 3 T for detection–histopathologic correlation. *Radiology* 2010 Apr;255(1):89-99.
9. Rosenkrantz AB, Mussi TC, Borofsky MS, Scionti SS, Grasso M, Taneja SS. 3.0 T multiparametric prostate MRI using pelvic phased-array coil: utility for tumor detection prior to biopsy. *Urologic Oncology* 2013 Nov;31(8):1430-5.
10. Hambrock T, Somford DM, Huisman HJ, van Oort IM, Witjes JA, Hulsbergen-van de Kaa CA, et al. Relationship between apparent diffusion coefficients at 3.0-T MR imaging and Gleason grade in peripheral zone prostate cancer. *Radiology* 2011 May;259(2):453-61.
11. Turkbey B, Shah VP, Pang Y, Bernardo M, Xu S, Kruecker J, et al. Is apparent diffusion coefficient

- associated with clinical risk scores for prostate cancers that are visible on 3-T MR images? *Radiology* 2011Feb;258(2):488-95.
12. Tamada T, Kanomata N, Sone T, Jo Y, Miyaji Y, Higashi H, et al. High b value (2,000 s/mm²) diffusion-weighted magnetic resonance imaging in prostate cancer at 3 Tesla: comparison with 1,000 s/mm² for tumor conspicuity and discrimination of aggressiveness. *PLOS ONE* 2014;9(5):e96619.
 13. Kitajima K, Takahashi S, Ueno Y, Yoshikawa T, Ohno Y, Obara M, et al. Clinical utility of apparent diffusion coefficient values obtained using high b-value when diagnosing prostate cancer using 3 tesla MRI: comparison between ultra-high b-value (2000 s/mm²) and standard high b-value (1000 s/mm²). *J Magn Reson Imaging* 2012Jul;36(1):198-205.
 14. Grant KB, Agarwal HK, Shih JH, Bernardo M, Pang Y, Daar D, et al. Comparison of calculated and acquired high b value diffusion-weighted imaging in prostate cancer. *Abdom Imaging* 2015;40:578-586.
 15. Bittencourt LK, Attenberger UI, Lima D, Strecker R, de Oliveira A, Schoenberg SO, et al. Feasibility study of computed vs measured high b-value (1400 s/mm²) diffusion-weighted MR images of the prostate. *World J Radiol* 2014 Jun 28;6(6):374-80.
 16. Rosenkrantz AB, Mannelli L, Kong X, Niver BE, Berkman DS, Babb JS, et al. Prostate cancer: utility of fusion of T2-weighted and high b-value diffusion-weighted images for peripheral zone tumor detection and localization. *J Magn Reson Imaging* 2011 Jul;34(1):95-100.
 17. Padhani AR, Liu G, Koh DM, Chenevert TL, Thoeny HC, Takahara T, et al. Diffusion-weighted magnetic resonance imaging as a cancer biomarker: consensus and recommendations. *Neoplasia* 2009 Feb;11(2):102-25.
 18. Maas MC, Futterer JJ, Scheenen TW. Quantitative evaluation of computed high B value diffusion-weighted magnetic resonance imaging of the prostate. *Invest Radiol* 2013Nov;48(11):779-86.
 19. Metens T, Miranda D, Absil J, Matos C. What is the optimal b value in diffusion-weighted MR imaging to depict prostate cancer at 3T? *European Radiol* 2012 Mar;22(3):703-9.
 20. Rosenkrantz AB, Hindman N, Lim RP, Das K, Babb JS, et al. Diffusion-weighted imaging of the prostate: comparison of b1000 and b2000 image sets for index lesion detection. *J Magn Reson Imaging* 2013;38:694-700
 21. Bieencourt LK, Attenberger UI, Lima D, Strecker R, de Oliveira A, et al. *World J Radiol* 2014(6); 374-380
 22. Medved M, Soyly-Boy FN, Karademir I, Sthei I, Yousef A, et al. High-resolution diffusion-weighted imaging of the prostate. *AJR* 2014;203:85-90
 23. Iwazawa J, Mitani T, Sassa S, Ohue S. Prostate cancer detection with MRI: is dynamic contrast-enhanced imaging necessary in addition to diffusion-weighted imaging? *Diagn Interv Radiol* 2011 Sep;17(3):243-8.
 24. Hoeks CM, Somford DM, van Oort IM, Vergunst H, Oddens JR, Smits GA, et al. Value of 3-T multiparametric magnetic resonance imaging and magnetic resonance-guided biopsy for early risk re-stratification in active surveillance of low-risk prostate cancer: a prospective multicenter cohort study. *Invest Radiol* 2014 Mar;49(3):165-72.

25. Vourganti S, Rastinehad A, Yerram NK, Nix J, Volkin D, Hoang A, et al. Multiparametric magnetic resonance imaging and ultrasound fusion biopsy detect prostate cancer in patients with prior negative transrectal ultrasound biopsies. *J Urol* 2012 Dec;188(6):2152-7.
26. Hegde JV, Chen MH, Mulkern RV, Fennessy FM, D'Amico AV, Tempany CM. Preoperative 3-Tesla multiparametric endorectal magnetic resonance imaging findings and the odds of upgrading and upstaging at radical prostatectomy in men with clinically localized prostate cancer. *Int J Radiat Oncol Biol Phys* 2013 Feb 1;85(2):e101-7.
27. Cornud F, Khoury G, Bouazza N, Beuvon F, Peyromaure M, Flam T, et al. Tumor target volume for focal therapy of prostate cancer-does multiparametric magnetic resonance imaging allow for a reliable estimation? *J Urol* 2014 May;191(5):1272-9.
28. Kuru TH, Roethke MC, Rieker P, Roth W, Fenchel M, Hohenfellner M, et al. Histology core-specific evaluation of the European Society of Urogenital Radiology (ESUR) standardized scoring system of multiparametric magnetic resonance imaging (mpMRI) of the prostate. *BJU international* 2013 Dec;112(8):1080-7.
29. Somford DM, Hamoen EH, Futterer JJ, van Basten JP, Hulsbergen-van de Kaa CA, Vreuls W, et al. The predictive value of endorectal 3 Tesla multiparametric magnetic resonance imaging for extraprostatic extension in patients with low, intermediate and high risk prostate cancer. *J Urol* 2013 Nov;190(5):1728-34.
30. Tamada T, Sone T, Higashi H, Jo Y, Yamamoto A, Kanki A, et al. Prostate cancer detection in patients with total serum prostate-specific antigen levels of 4-10 ng/mL: diagnostic efficacy of diffusion-weighted imaging, dynamic contrast-enhanced MRI, and T2-weighted imaging. *Am J Roentgenology* 2011 Sep;197(3):664-70.
31. Miller GJ, Cygan JM. Morphology of prostate cancer: the effects of multifocality on histological grade, tumor volume and capsule penetration. *JURO* 1994 Nov;152(5 Pt2):1709-13.
32. Arora R, Koch MO, Eble JN, Ulbright TM, Li L, Cheng L. Heterogeneity of Gleason grade in multifocal adenocarcinoma of the prostate. *Cancer* 2004;100(11):2362-6.
33. Karavitakis M, Ahmed HU, Abel PD, Hazell S, Winkler MH. Margin status after laparoscopic radical prostatectomy and the index lesion: implications for preoperative evaluation of tumor focality in prostate cancer. *Journal of Endourology* 2012 May;26(5):503-8.
34. Algaba F, Montironi R. Impact of prostate cancer multifocality on its biology and treatment. *Journal of Endourology* 2010 May;24(5):799-804.
35. Wise AM, Stamey TA, McNeal JE, Clayton JL. Morphologic and clinical significance of multifocal prostate cancers in radical prostatectomy specimens. *Urology* 2002 Aug;60(2):264-9.
36. Epstein JI. Prognostic significance of tumor volume in radical prostatectomy and needle biopsy specimens. *The Journal of Urology*. 2011 Sep;186(3):790-7.
37. van der Kwast TH, Amin MB, Billis A, Epstein JI, Griffiths D, Humphrey PA, et al. International Society of Urological Pathology (ISUP) Consensus Conference on Handling and Staging of Radical Prostatectomy Specimens. Working group 2: T2 substaging and prostate cancer volume. *Modern Pathology* Nature Publishing Group; 2010 Sep 3;24(1):16-25.
38. Rud E, Klotz D, Rennesund K, Baco E, Berge V, Lien D, Svindland A, Lundeby E, Berg RE, Eri LM,

- Eggesbø HB. Detection of the Index Tumor and Tumor Volume in Prostate Cancer using T2w and DW MRI alone. *BJU Int* 2014;114:E32-E42.
39. Ward E, Baad M, Peng Y, Yousuf A, Wang S, Antic T, et al. Multi-parametric MR imaging of the anterior fibromuscular stroma and its differentiation from prostate cancer. *Abdom Radiol (NY)*. 2017;42:926-934.
 40. Bouye S, Potiron E, Puech P, Leroy X, Lemaitre L, Villers A. Transition zone and anterior stromal prostate cancers: zone of origin and intraprostatic patterns of spread at histopathology. *The Prostate*. 2009;69:105-113.
 41. Junker D, Steinkohl F, Fritz V, Bektic J, Tokas T, Aigner F, et al. Comparison of multiparametric and biparametric MRI of the prostate: are gadolinium-based contrast agents needed for routine examinations? *World journal of urology*. 2018
 42. Sun C, Chatterjee A, Yousuf A, Antic T, Eggner S, Karczmar GS, Oto A. Comparison of T2-Weighted Imaging, DWI, and Dynamic Contrast-Enhanced MRI for Calculation of Prostate Cancer Index Lesion Volume: Correlation With Whole-Mount Pathology. *AJR Am J Roentgenol*. 2019;212:351-356

SECTION V: STAGING

1. Engelbrecht MR, Jager GJ, Laheij RJ, Verbeek AL, van Lier HJ, Barentsz JO. Local staging of prostate cancer using magnetic resonance imaging: a meta-analysis. *European Radiol* 2002Sep;12(9):2294-302.
2. Johnston R, Wong LM, Warren A, Shah N, Neal D. The role of 1.5 Tesla magnetic resonance imaging in staging prostate cancer. *ANZ J Surg* 2013 Apr;83(4):234-8.
3. Wang L, Mullerad M, Chen HN, Eberhardt SC, Kattan MW, Scardino PT, Hricak H. Prostate cancer: incremental value of endorectal MR imaging findings for prediction of extracapsular extension. *Radiology* 2004;232:133-9.
4. Renard-Penna R, Roupret M, Comperat E, Ayed A, Coudert M, Mozer P, et al. Accuracy of high resolution (1.5 tesla) pelvic phased array magnetic resonance imaging (MRI) in staging prostate cancer in candidates for radical prostatectomy: results from a prospective study. *Urologic Oncology* 2013 May;31(4):448-54.
5. Thoeny HC, Froelich JM, Triantafyllou M, Huesler J, Bains LJ, et al. Metastases in norma-sized pelvic lymph nodes: detection with diffusion-weighted MR imaging. *Radiology* 2014;273:125-135
6. Baco E, Rud E, Vlatkovic L, Svindland A, Eggesbø HB, Hung AJ, et al. Predictive value of Magnetic Resonance Imaging Determined Tumor Contact Length for Extra-capsular Extension of Prostate cancer. *J Urol* 2015;193:466-472.
7. Akin O, Sala E, Moskowitz CS, Kuroiwa K, Ishill NM, Pucar D, et al. Transition zone prostate cancers: features, detection, localization, and staging at endorectal MR imaging. *Radiology* 2006 Jun;239(3):784-792.

SECTOR MAP CREDIT

The prostate sector map was modified by David A. Rini, Department of Art as Applied to Medicine, Johns Hopkins University. It is based on previously published figures by Villers et al (*Curr Opin Urol* 2009;19:274-82) and Dickinson et al (*Eur Urol* 2011;59:477-94) with anatomical correlation to the normal histology of the prostate by McNeal JE (*Am J Surg Pathol* 1988 Aug;12:619-33).

FIGURES

Figure 1 – Anatomy of the prostate illustrated on T2-weighted imaging



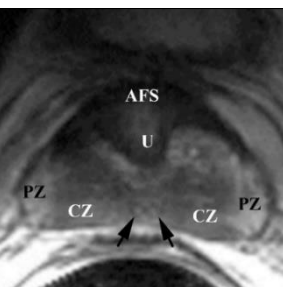
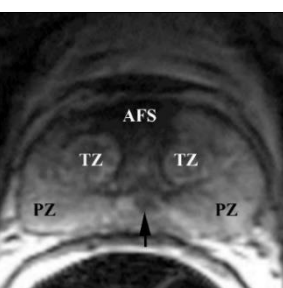
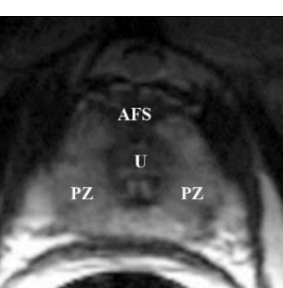
	<p>A. Sagittal image of the prostate shows the urethra (U), the course of ejaculatory duct (arrow) and the level of verumontanum (*) where the ejaculatory ducts merge and enter the mid prostatic urethra.</p>
	<p>B. Coronal image of the posterior prostate illustrates the central zone (CZ) and peripheral zone (PZ). Note that CZ has the shape of an inverted cone with its base oriented towards the base of the gland and is homogeneously hypointense as it contains more stroma than glandular tissue. CZ is well seen in younger patients; however age-related expansion of the transition zone by benign prostatic hyperplasia (BPH) may result in compression and displacement of the CZ leading to its poor visibility.</p>
	<p>C. Axial image of the prostate base, that constitutes the upper 1/3 of the gland just below the urinary bladder, shows the following anatomical zones: anterior fibromuscular stroma (AFS) containing smooth muscle, which mixes with muscle fibers around the urethra (U) at the bladder neck and contains no glandular tissue, hence it is markedly hypointense; central zone (CZ) surrounding the ejaculatory ducts (arrows); and peripheral zone (PZ) that covers the outer lateral and posterior regions of the prostate.</p>
	<p>D. Axial image of the midgland, that constitutes the middle 1/3 of the prostate and includes verumontanum in the mid prostatic urethra, shows anterior fibromuscular stroma (AFS) and transition zone (TZ) tissue around the urethra. Note increasing volume of peripheral zone (PZ) in the midgland where it occupies the outer lateral and posterior regions of the prostate and is homogeneously hyperintense. Arrow points to converging ejaculatory ducts as they enter the mid prostatic urethra at verumontanum.</p>
	<p>E. Axial image of the apex of the prostate, that constitutes the lower 1/3 of the prostate, shows hypointense anterior fibromuscular stroma (AFS) in front of the urethra (U). Peripheral zone (PZ) makes up most of the apex of the prostate.</p>

Figure 2 – PI-RADS assessment for peripheral zone on T2-weighted imaging.

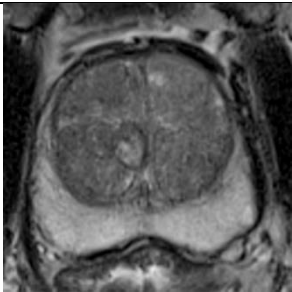

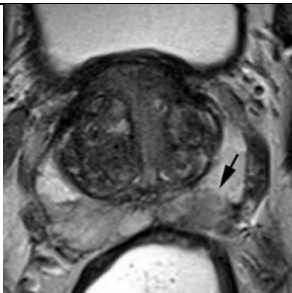
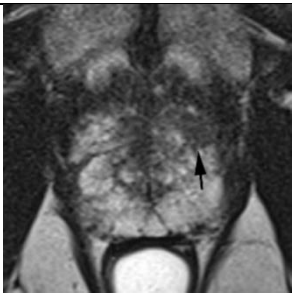
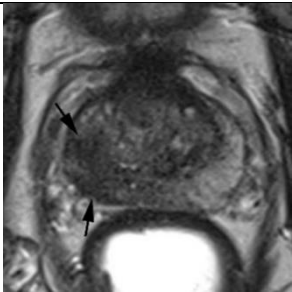
1		Uniform hyperintense signal intensity (normal).
2		Linear (arrow), wedge-shaped, or diffuse mild hypointensity, usually indistinct margin.
3		Heterogeneous signal intensity or non-circumscribed, rounded, moderate hypointensity (arrow).
4		Circumscribed, homogenous moderate hypointense focus/mass confined to prostate and <1.5 cm in greatest dimension (arrow).
5		Same as 4 but ≥ 1.5 cm in greatest dimension (arrows) or definite extraprostatic extension/invasive behavior.

Figure 3 – PI-RADS assessment for transition zone on T2-weighted imaging.

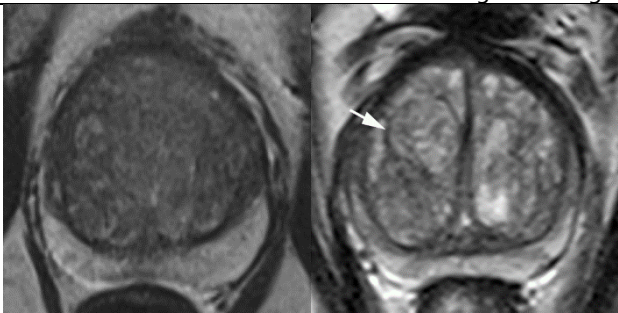
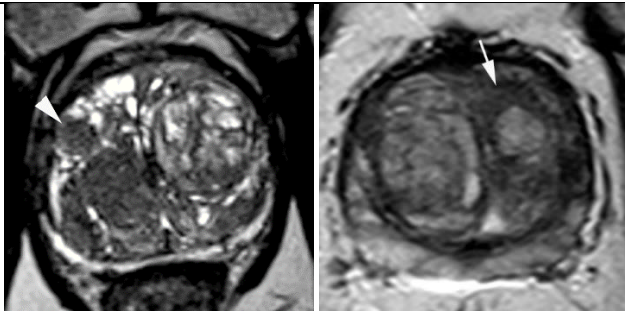
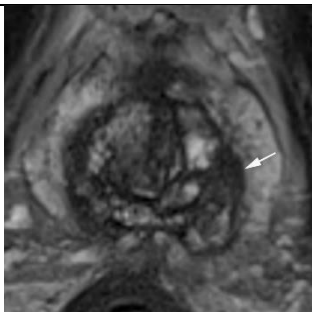
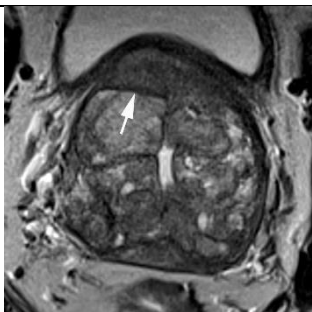

1		Normal appearing TZ (rare) - homogeneous intermediate signal intensity, OR a round, completely encapsulated (arrow) nodule ("typical nodule")
2		A mostly encapsulated nodule OR a homogeneous circumscribed nodule without encapsulation (arrowhead) ("atypical nodule") OR a homogeneous mildly hypointense area between nodules (arrow)
3		Heterogeneous signal intensity with obscured margins (arrow). Includes others that do not qualify as 2, 4, or 5.
4		Lenticular (arrow) or non-circumscribed, homogeneous, moderately hypointense, and <1.5 cm in greatest dimension.
5		Same as 4, but ≥ 1.5 cm in greatest dimension (arrows) or definite extraprostatic extension/invasive behavior.

Figure 4 – PI-RADS assessment for peripheral zone on diffusion weighted imaging

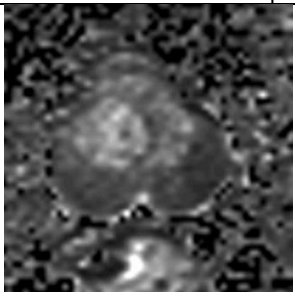

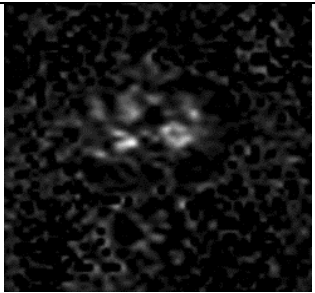

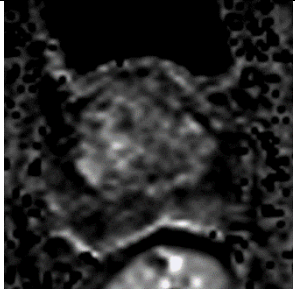

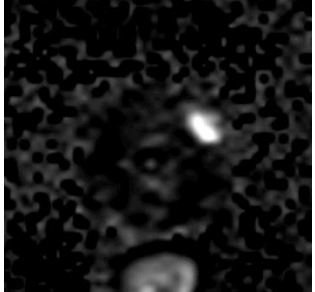
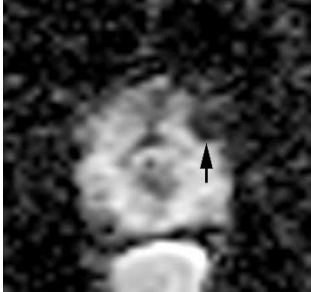
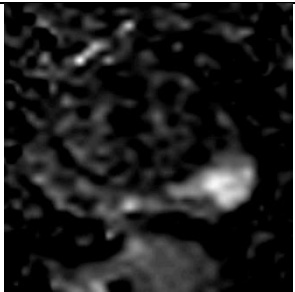
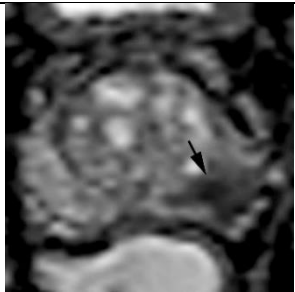
1			No abnormality (i.e. normal) on ADC and high b-value DWI.
2			Linear/wedge shaped hypointense on ADC and/or linear/wedge shaped hyperintense on high b-value DWI
3			Focal (discrete and different from the background) hypointense on ADC and/or focal hyperintense on high b-value DWI; may be markedly hypointense on ADC or markedly hyperintense on high b-value DWI, but not both.
4			Focal markedly hypointense on ADC and markedly hyperintense on high b-value DWI; <1.5cm in greatest dimension
5			Same as 4 but ≥1.5cm in greatest dimension or definite extraprostatic extension/invasive behavior
	High b-value DWI	ADC map	

Figure 5 – PI-RADS assessment for transition zone on diffusion weighted imaging.


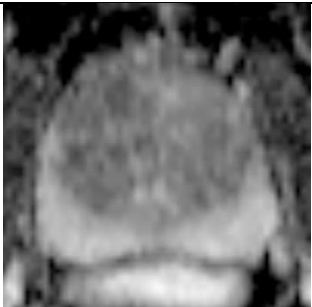


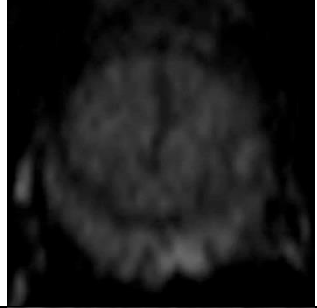
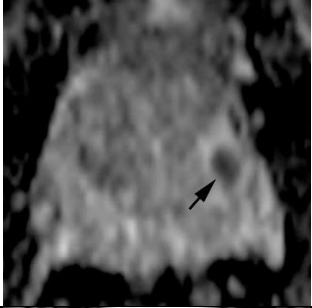


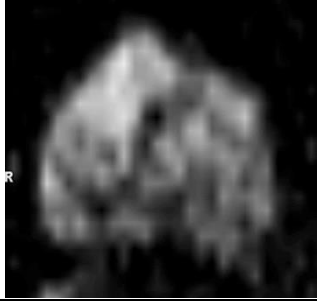
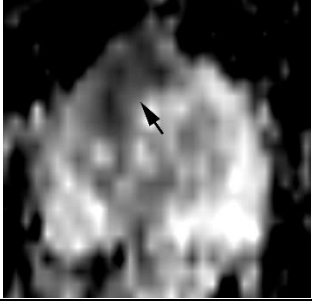
1			No abnormality (i.e. normal) on ADC and high b-value DWI
2			Linear/wedge shaped hypointense on ADC and/or linear/wedge shaped hyperintense on high b-value DWI Non-focal hypointense on ADC and/or hyperintense on high b-value DWI
3			Focal (discrete and different from the background) hypointense on ADC (arrow) and/or focal hyperintense on high b-value DWI; may be markedly hypointense on ADC OR markedly hyperintense on high b-value DWI, but <u>not both</u>
4			Focal markedly hypointense on ADC AND markedly hyperintense on high b-value DWI; <1.5cm in greatest dimension
5			Same as 4 but ≥1.5cm in greatest dimension or definite extraprostatic extension/invasive behavior
	High b-value DWI	ADC map	

Figure 6 – PI-RADS assessment for dynamic contrast enhanced MRI.

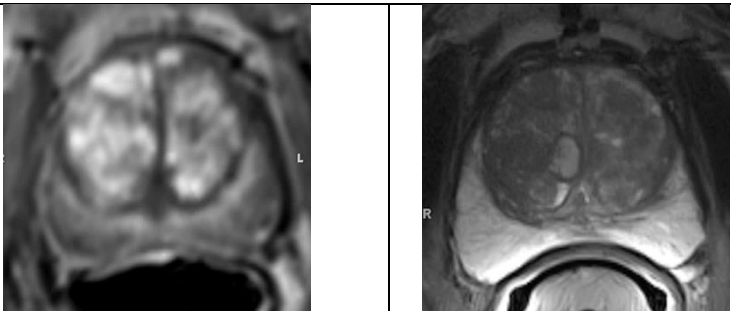
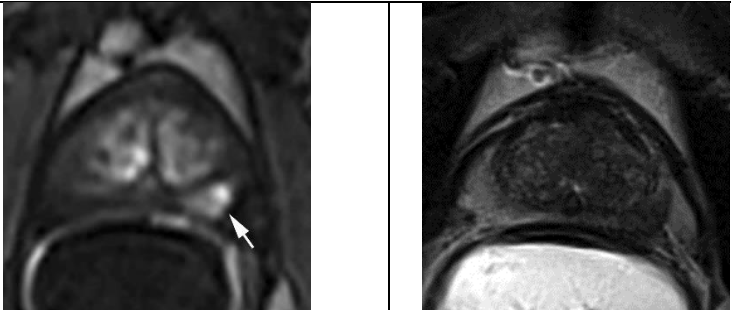
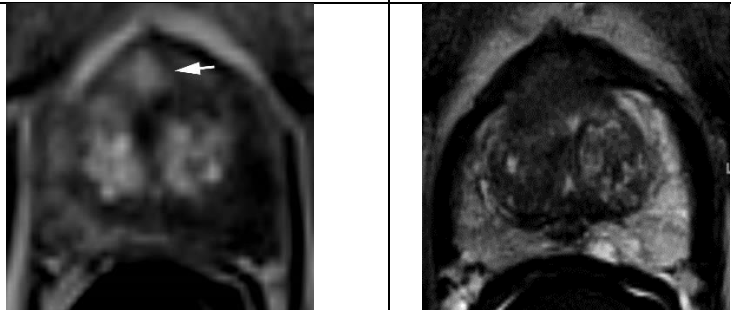
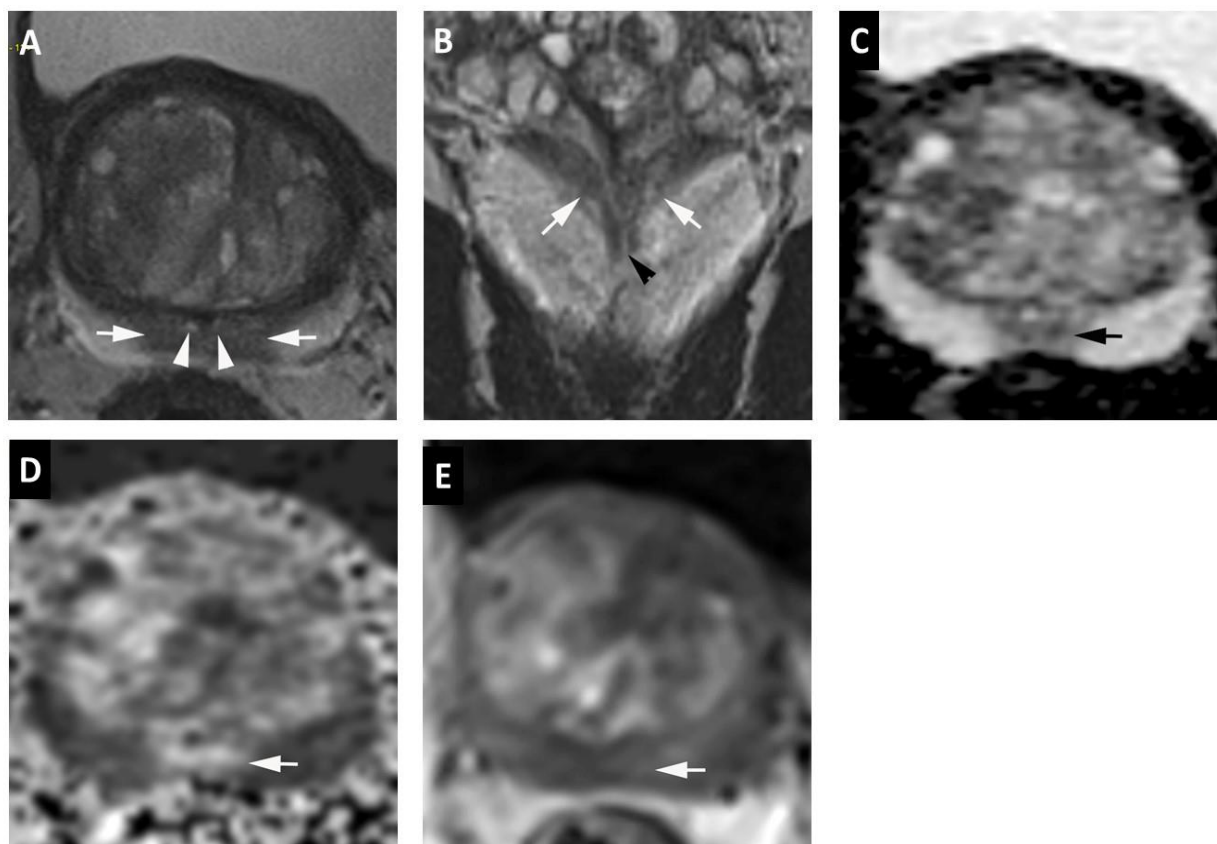
Negative		
	<p>No early or contemporaneous enhancement; or diffuse multifocal enhancement NOT corresponding to a focal finding on T2W and/or DWI or focal enhancement corresponding to a lesion demonstrating features of BPH on T2WI (including features of extruded BPH in the PZ)</p>	
Positive		
		
	<p>Focal, and; earlier than or contemporaneously with enhancement of adjacent normal prostatic tissues, and; corresponds to suspicious finding on T2W and/or DWI</p>	

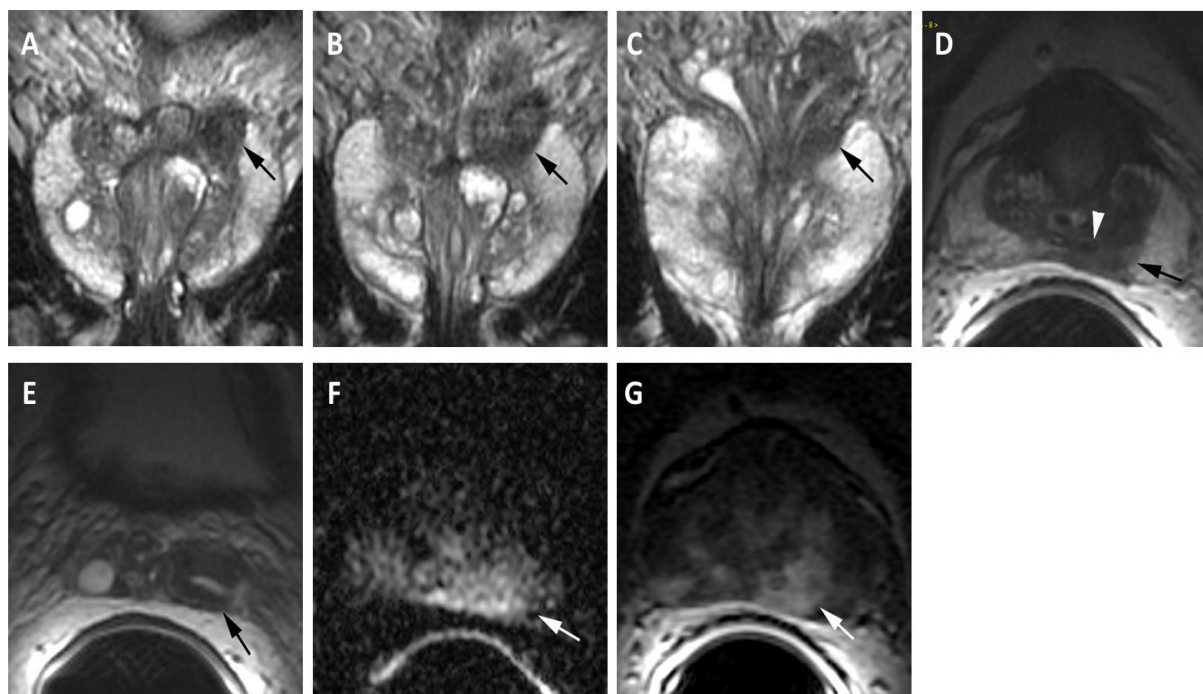
Figure 7 – Normal Central Zone.



- A. Axial T2-weighted image shows symmetric homogeneous hypointense signal (arrows) surrounding the ejaculatory ducts (arrowheads) at the prostate base.
- B. Coronal T2-weighted image shows symmetric homogeneous hypointense signal (arrows) in a cone-shaped distribution extending from the base to the level of verumontanum (arrowhead) in the mid gland.
- C. Axial ADC map shows symmetric mildly hypointense signal corresponding to A. (arrow).
- D. Diffusion-weighted image ($b=1400 \text{ sec/mm}^2$) shows symmetric mildly hyperintense signal intensity corresponding to A. and B. (arrow).
- E. Early dynamic contrast enhanced image shows no enhancement in the region of the central zone (arrow).

T2W MRI PI-RADS=1, DWI PI-RADS=1, DCE-MRI PI-RADS=negative,
PI-RADS Assessment Category=1

Figure 8- Central Zone Prostate Cancer



MRI performed at 1.5T with endorectal coil in a 59-year-old man with prostate cancer (radical prostatectomy adenocarcinoma showing Gleason 4+3 prostate cancer in the left base with extraprostatic extension and left seminal vesicle invasion).

A-C. Coronal T2-weighted images show asymmetric T2 moderately hypointense signal intensity involving the left base with extension into the left seminal vesicle (arrow).

D. Axial T2-weighted image shows asymmetric T2 moderately hypointense signal intensity (arrow) in the left central zone surrounding the left ejaculatory duct (arrowhead).

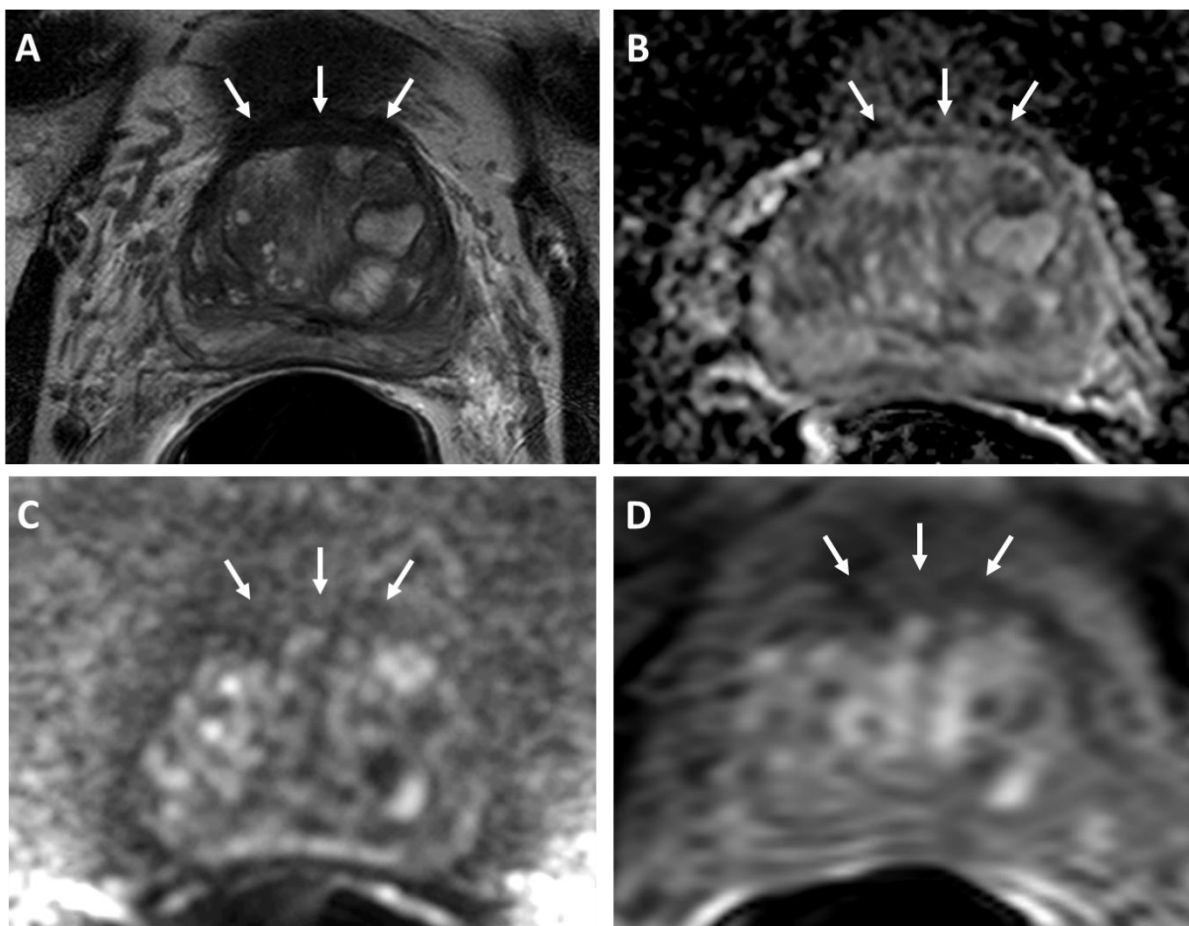
E. Axial T2-weighted image shows asymmetric thickening of the wall of left seminal vesicle (arrow).

F. Axial diffusion weighted image (b=1000 sec/mm²) shows asymmetric hyperintense signal intensity in the left central zone.

G. Axial dynamic contrast-enhanced image shows early intense asymmetric enhancement corresponding to signal abnormalities on T2W and DW images.

T2W MRI PI-RADS=5, DWI PI-RADS=5, DCE-MRI PI-RADS=positive,
PI-RADS Assessment Category= 5.

Figure 9. Normal Anterior Fibromuscular Stroma (AFMS).



Normal anterior fibromuscular stroma (AFMS) is composed of vertically oriented smooth muscle bundles continuous with the bladder smooth muscle and covers the anterior surface of the prostate as a non-glandular layer.

A. Axial T2-weighted image shows symmetric markedly hypointense signal intensity along the anterior aspect of the prostate, typical of normal AFMS (arrows).

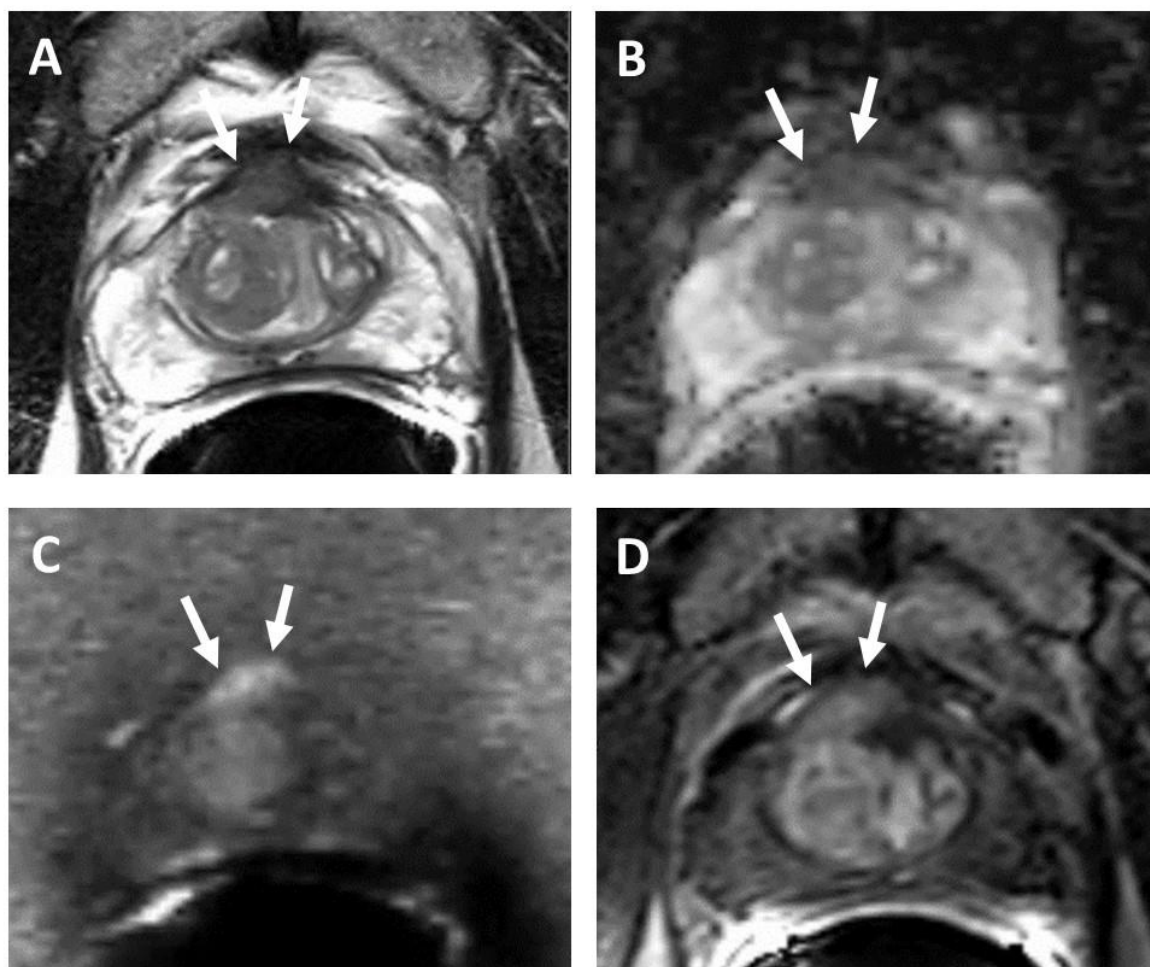
B. Axial ADC map shows normal signal intensity (similar to that of the background prostate) along the AFMS, which is typical of normal AFMS (arrows).

C. Diffusion-weighted image (b=2000sec/mm²) shows normal hypointense signal intensity (similar to that of the background prostate) along the AFMS (arrows).

D. Early dynamic contrast enhanced image shows lack of enhancement along the AFMS (arrows).

T2W MRI PI-RADS=1, DWI PI-RADS=1, DCE-MRI PI-RADS=negative,
Overall PI-RADS=1

Figure 10: Prostate Cancer Appearing to Involve the Anterior Fibromuscular Stroma

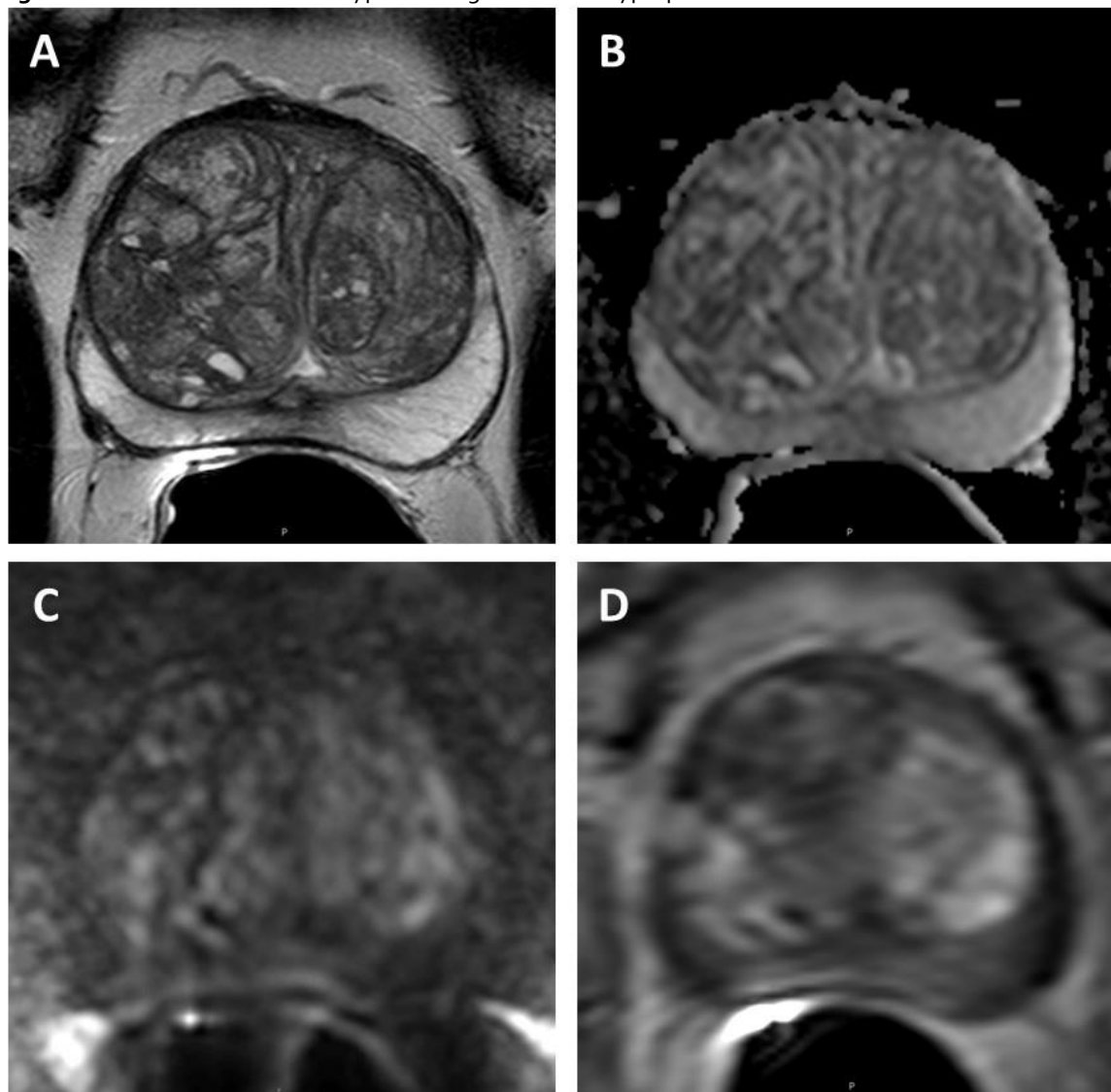


Prostate cancer appearing to involve the anterior fibromuscular stroma and thus scored using transition zone criteria. 68-year-old man with PSA 4.1 ng/mL and Gleason score 3+4 prostate cancer confirmed on MRI guided targeted biopsy.

- A. Axial T2-weighted image shows a lenticular homogeneous moderately T2 hypointense lesion (arrows) appearing to involve the anterior fibromuscular stroma with extraprostatic extension.
- B. ADC map shows focal hypointense signal intensity lesion corresponding to A. (arrows).
- C. Diffusion-weighted image (b=2000sec/mm²) shows markedly hyperintense signal intensity (arrows) corresponding to A and B.
- D. Early dynamic contrast enhanced image shows avid enhancement within the anterior lesion (arrows).

T2W MRI PI-RADS=5, DWI PI-RADS=5, DCE-MRI PI-RADS=positive,
PI-RADS Assessment Category=5

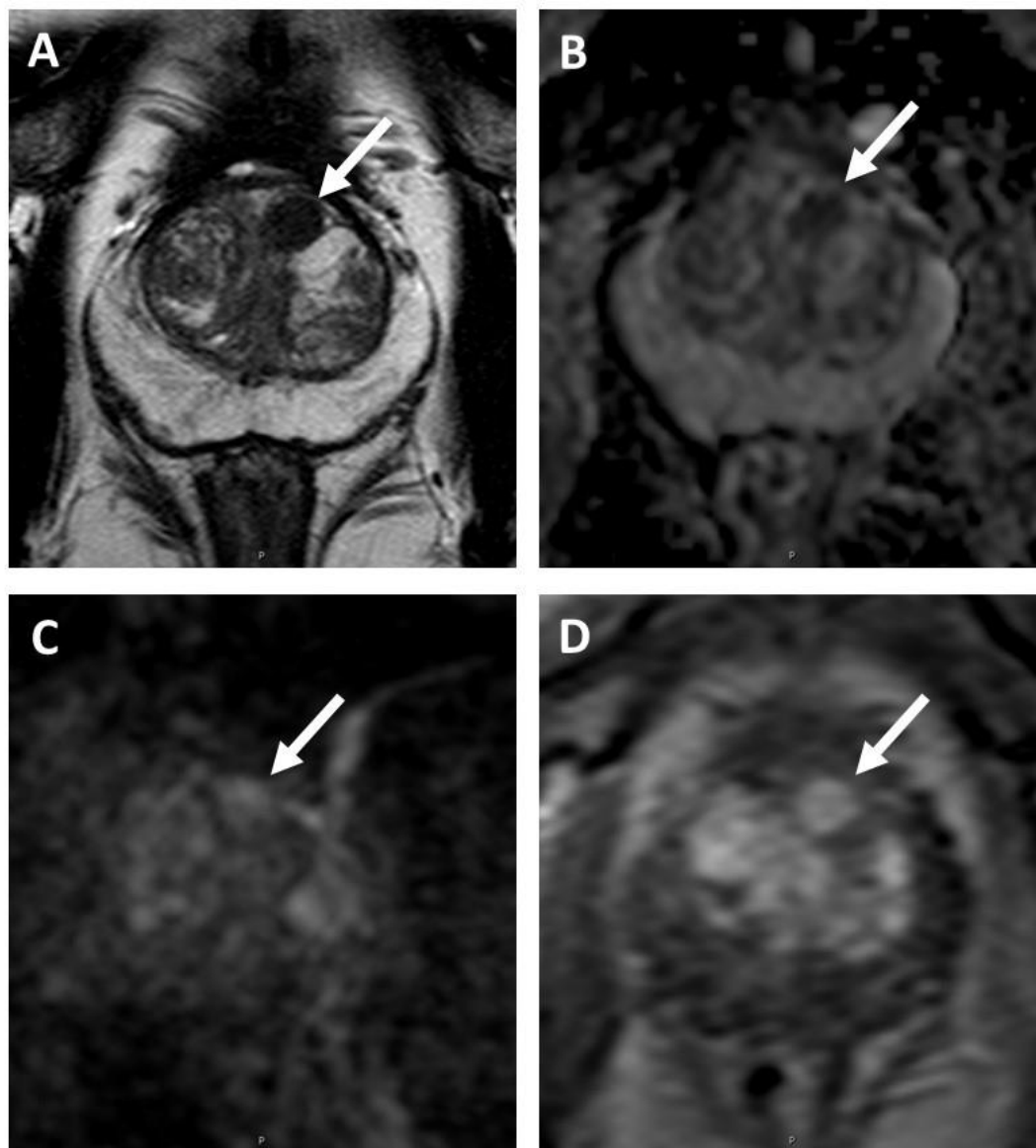
Figure 11. Transition Zone with Typical Benign Prostatic Hyperplasia.



- A. Axial T2-weighted image shows completely encapsulated “typical” nodules creating the “organized chaos” pattern.
- B. ADC map shows no focal lesion with low signal intensity below the background.
- C. Diffusion-weighted image (b-2000sec/mm²) shows no lesion with markedly hyperintense signal above the background.
- D. Early dynamic contrast enhanced image shows avid enhancement within the typical BPH nodules.

T2W MRI PI-RADS=1, DWI PI-RADS=1, DCE-MRI PI-RADS=negative,
PI-RADS Assessment Category=1

Figure 12. Transition Zone with an Atypical Nodule.



A. Axial T2-weighted image shows a homogeneous T2 hypointense mostly encapsulated nodule (arrow).

B. ADC map shows focal lesion with markedly hypointense signal intensity below background corresponding to the lesion seen in A (arrow).

C. Diffusion-weighted image (b=1500sec/mm²) shows focal lesion with markedly hyperintense signal intensity above background (arrow) corresponding to the lesion seen in A and B.

D. Early dynamic contrast enhanced image shows avid enhancement within the nodule (arrow).

T2W MRI PI-RADS=2, DW PI-RADS=4, DCEMRI PI-RADS=positive,
PI-RADS Assessment Category=3

Figure 13. Schematic diagram of features of nodules in the TZ and their corresponding scores. Assessment of nodule shape and margins should be done in at least two planes. Oval or spherical shape and cystic change are acceptable features within nodules.

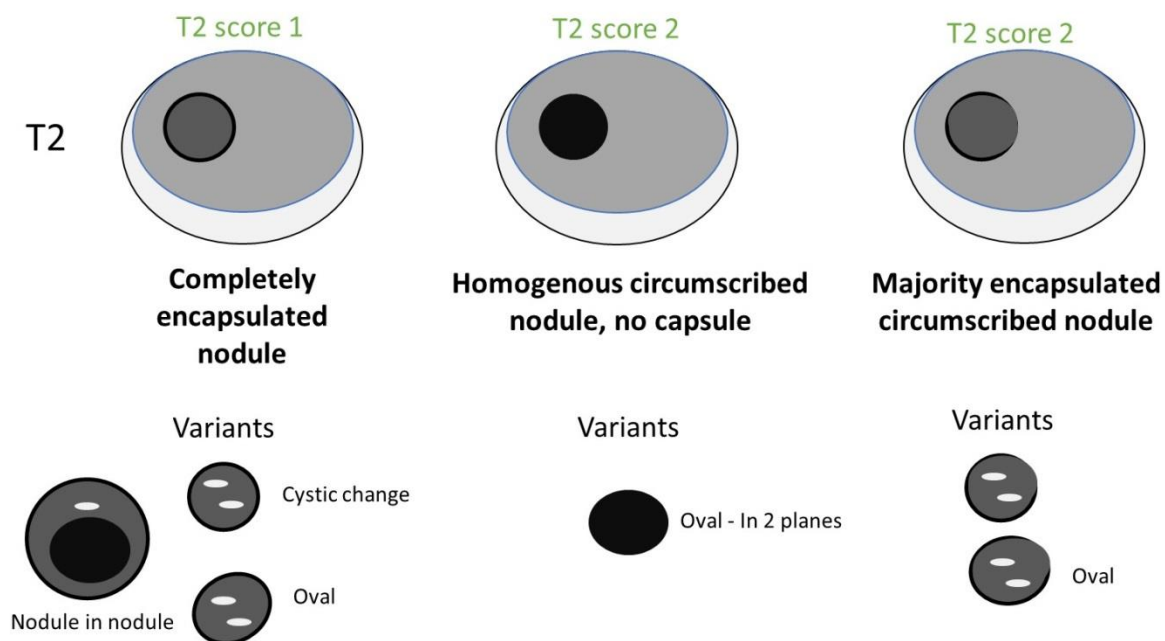


Figure 14. Schematic diagram of PI-RADS v2.1 scoring for TZ that incorporates DWI for determination of assessment category for partially encapsulated or circumscribed, non-encapsulated nodules with clearly restricted (impeded) diffusion (DWI score 4 or 5) is scored a 3 (dotted lines indicate the region of a near isointense lesion where the borders are indistinct or difficult to define because of the near isointensity).

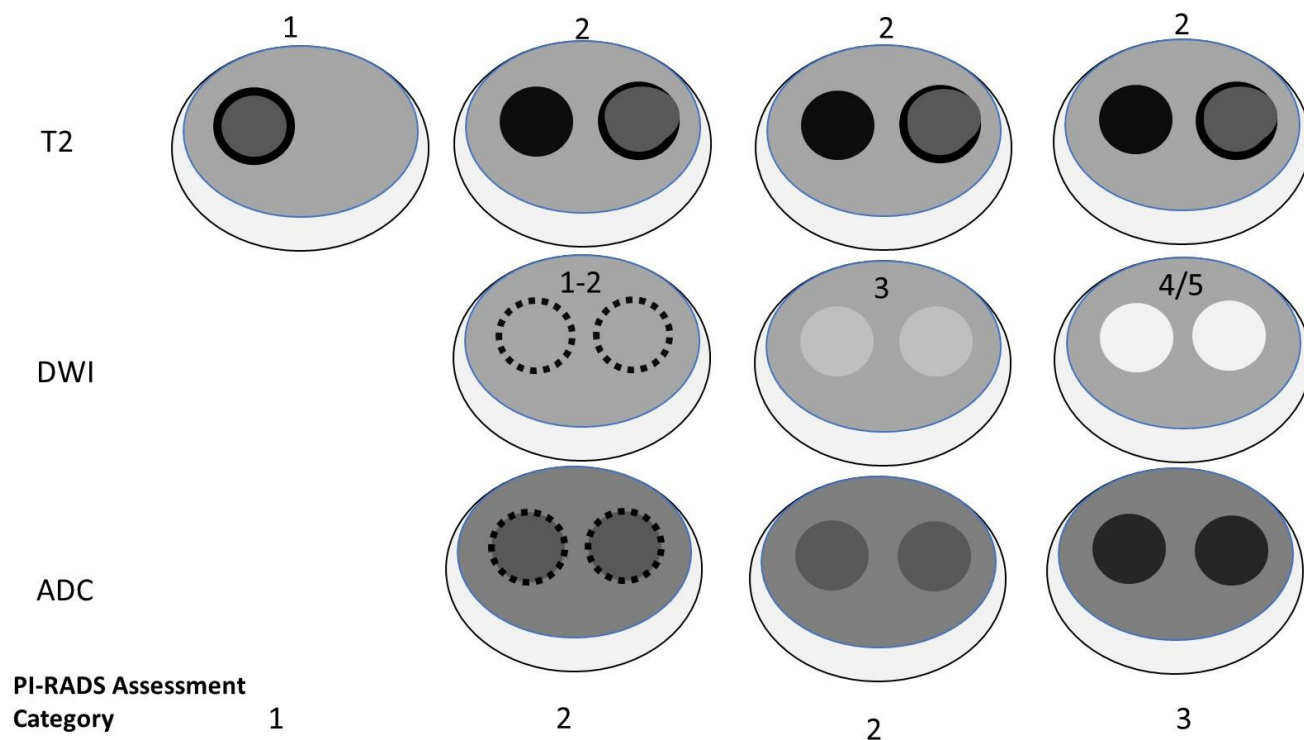
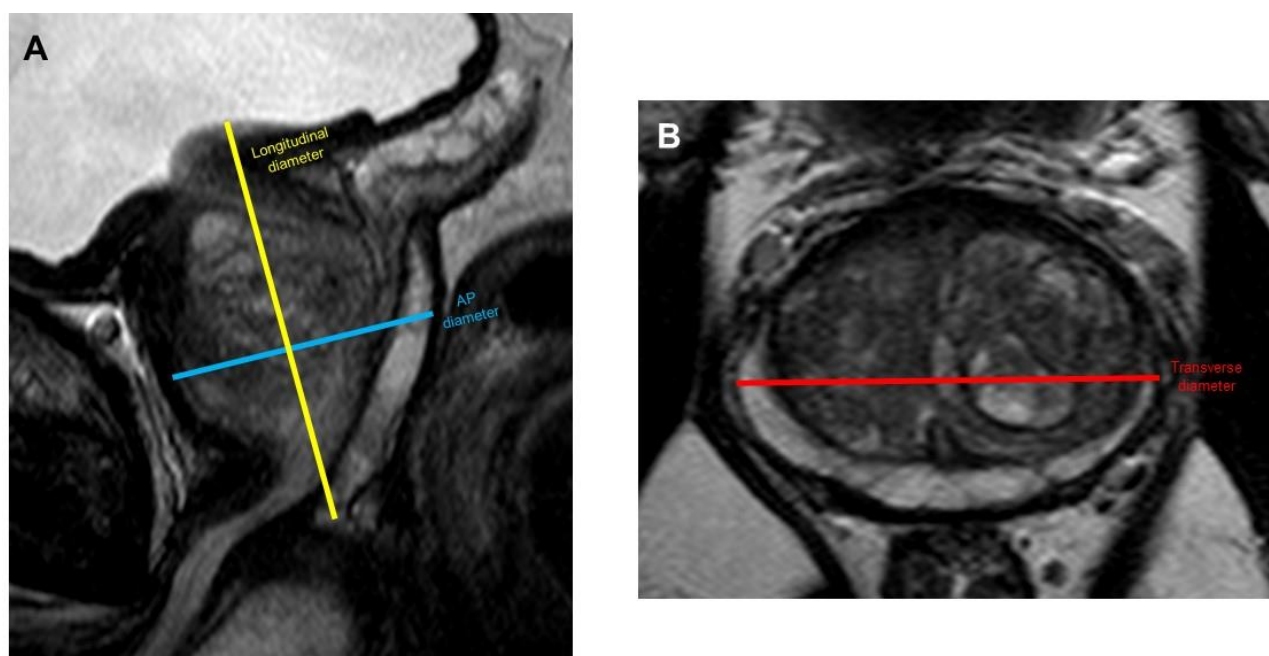
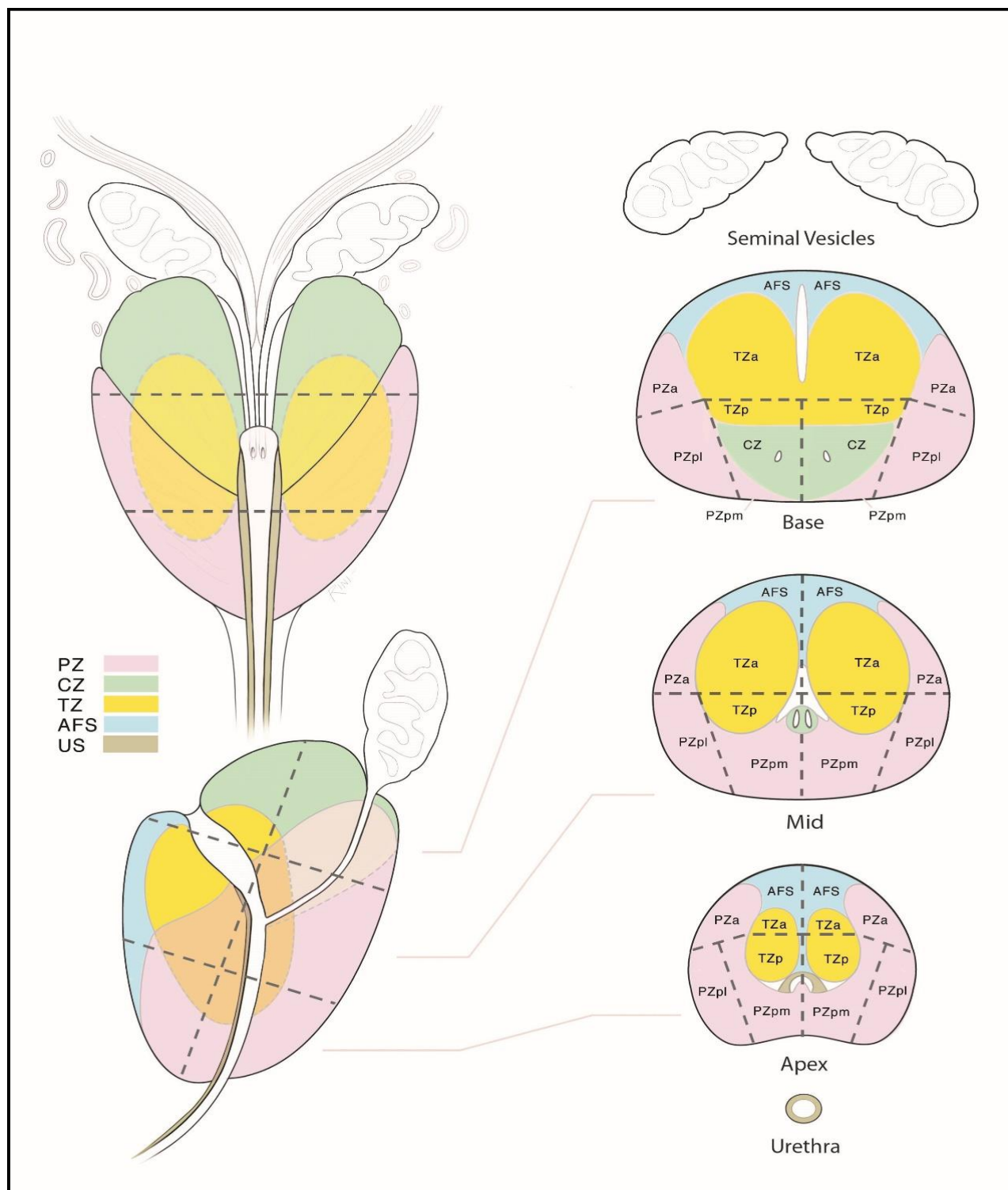


Figure 15. Suggested Measurements for Ellipsoid Formula when Calculating Prostate Volume at MRI.



Maximum longitudinal diameter and maximum AP diameter should be measured on mid sagittal T2W MRI (A), whereas maximum transverse diameter should be measured on axial T2W MRI (B).

Figure 16: Sector map diagram v2.1.



The segmentation model used in PI-RADS v2.1 employs thirty-eight sectors/regions for the prostate, two for the seminal vesicles and one for the membranous urethra (Total 41).

The right and left peripheral zones (PZ) at prostate base, mid-gland, and apex are each subdivided into three sections: anterior (a), posterior medial (pm), and posterior lateral (pl).

The right and left transition zones (TZ) at prostate base, mid-gland, and apex are each subdivided into two sections: anterior (a) and posterior (p).

The anterior fibromuscular stroma (AFS) is divided into right/left at the prostate base, midgland, and apex.

The seminal vesicles (SV) are divided into right/left.

The sector map illustrates an idealized prostate. Since the prior version, in addition to two new sectors at the base there have been adjustments to the location of ejaculatory ducts, angulation of the proximal urethra, and overall proportions of the gland to match between the coronal, sagittal, and axial images. In patients and their corresponding MR images, most prostates have anatomical components that are enlarged or atrophied, and the PZ may be obscured by an enlarged TZ, and CZ may not be easily identifiable. In such instances, a diagram is used as an approximation of the gland and a sector map can be marked to indicate the location of the findings in addition to the written report.

Diagram credit: The prostate sector diagram was modified by DAVID A. RINI, MFA, CMI, FAMI, Associate Professor in the Department of Art as Applied to Medicine at the Johns Hopkins University, based on previously published figures by Villers et al (Curr Opin Urol. 2009;19:274-82) and Dickinson et al (Eur Urol. 2011;59:477-94) with anatomical correlation to the normal histology of the prostate by McNeal JE (Am J Surg Pathol. 1988 Aug;12:619-33)

Figures were modified from PI-RADS version 2.0 and Prostate Imaging Reporting and Data System Version 2.1: 2019 Update of Prostate Imaging Reporting and Data System Version 2. European Urology 2019

DOI: <https://doi.org/10.1016/j.eururo.2019.02.033>